Parametrization of the cumulant lattice Boltzmann method for fourth order accurate diffusion Part I: Derivation and validation

Article *in* Journal of Computational Physics · July 2017

DOI: 10.1016/j.jcp.2017.05.040

CITATIONS
2

READS
267

3 authors:

Martin Geier
Technische Universität Braunschweig
35 PUBLICATIONS **364** CITATIONS
SEE PROFILE

Andrea Pasquali
FluiDyna GmbH
8 PUBLICATIONS **50** CITATIONS
SEE PROFILE

Martin Schönherr
Technische Universität Braunschweig
10 PUBLICATIONS **107** CITATIONS
SEE PROFILE

Parametrization of the cumulant lattice Boltzmann method for fourth order accurate diffusion Part I: derivation and validation[1]

Martin Geier[a,*], Andrea Pasquali[a,b], Martin Schönherr[a]

[a] *TU Braunschweig, Institute for Computational Modeling in Civil Engineering (iRMB),Braunschweig, Germany*
[b] *FluiDyna GmbH, Unterschleissheim, Germany*

Abstract

The cumulant lattice Boltzmann method offers a set off free relaxation parameters that do not influence the result at leading order but can be used to influence the leading error. Using Taylor expansion we derive exact functional relationships for the elimination of the linearized leading error of the method. The diffusion term in the Navier-Stokes equation becomes fourth order accurate for small enough viscosity with these parameters. The result is general and does not depend on the flow. The analytical solution is tested against Taylor-Green vortex flow and shear wave flow and fourth order accuracy for the diffusion is observed.

Keywords: lattice Boltzmann, cumulants, quartic parameters, multiple relaxation times, fourth order

1. Introduction

Solving the Navier-Stokes equation at high Reynolds numbers is a problem of significant industrial importance. At the same time it is among the computationally most demanding tasks. The progress in computational hardware, while being impressive, is still insufficient for meeting the demand. Therefore, researchers seek ways to improve the efficiency of their computational methods. In this regard, measures that increase the convergence order of a numerical method are among the most interesting as they promise to make the best use of computational resources. This is especially so if they are combined with large computational resources and applied at high resolution. On the other hand, increasing the convergence order of a numerical method usually involves a steep increase in the complexity of the model. In the case of stencil based methods, larger neighborhoods are usually required to increase the convergence order. In this paper we evaluate the possibility to improve the convergence order of the lattice Boltzmann method without increasing the size of the stencil and at minimal computational overhead. We derive a parametrization that improves the convergence for the diffusion term in the Navier-Stokes equation modeled by the cumulant lattice Boltzmann method to fourth order for sufficiently low viscosity.

It is known for some time [1] that lattice Boltzmann schemes with multiple relaxation times (MRT) [2, 3, 4] offer a parametrization where the numerical error, either for the Navier-Stokes, the Stokes or the advection diffusion equation, for steady solutions at fixed resolution becomes a function of a certain combination of odd and even relaxation rates [5]. Keeping this combination fixed makes the error independent of the transport coefficients, such as viscosity or heat conductivity. This principle has first been applied by Ginzburg and Adler [6] to investigate the apparent dependence of boundary locations for simple boundary conditions. Later, more advanced boundary conditions were derived that apply the parametrization to obtain very accurate solutions [7, 8, 9, 5].

From the finding that the errors depend only on a specific, so-called magic parameter [1] naturally arises the question whether this dependence can be made to zero at any predefined asymptotic order, i.e. whether it is possible to turn a second order numerical scheme, such as the lattice Boltzmann method, into a fourth order accurate scheme

[1] accepted by Journal of Computational Physics 2017
*Corresponding author at: iRMB Pockelsstr. 3, 38106 Braunschweig, Germany. Tel: +49 531 391 94518; Fax: +49 531 391 94511.
Email address: geier@irmb.tu-bs.de (Martin Geier)

by means of a simple parametrization. Some progress has indeed been made in this regard [10, 11] but most work in the field was devoted to Stokes-like equations [12] and advection diffusion equations [13, 14] including anisotropic diffusion [15, 16, 17]. So far, the work on magic parameters bears little relevance for turbulent flow simulations. In particular, turbulent flow is never steady. Also, the insight into the accuracy gains for boundary conditions by using magic parameters diminishes in significance at low enough viscosity, and therefore high enough Reynolds numbers, as these errors are proportional to viscosity squared [1] in the BGK-form of the collision operator.

If we want to apply the method of magic parameters to turbulent flow simulations we have to take the influence of the use of several independent relaxation parameters on the non-linear advection into consideration. In this regard it is of note that different incompatible magic parameters were found for the elimination of the leading order error in steady state advection and in diffusion [15]. Further it was found that these solutions could be generalized to transient flows only when combined with specific transport coefficients [15, 16].

It has been shown by us [18] that the original MRT ansatz with moments derived in a fixed reference frame breaks Galilean invariance whenever certain relaxation rates are not coupled. This is an obstacle in the search for a parametrization of the method that improves convergence. Improving the accuracy in diffusion has an impact on advection. To overcome this problem we proposed the cumulant lattice Boltzmann method [18] for which the choice of relaxation rates is neutral to Galilean invariance and hence advection.

The cumulant lattice Boltzmann model uses statistically independent observable quantities (cumulants) instead of moments as the degrees of freedom in the collision [18, 19, 20, 21, 22, 23]. In its original presentation all relaxation rates not related to shear viscosity were set to unity in [18]. We noted that this might not be the optimal choice. In the current paper we will derive optimal values for some of the undetermined relaxation rates. Given the fact that the cumulant lattice Boltzmann method has the maximal number of free parameters and given that the constraints between that parameters in the classical MRT method have been removed, the cumulant lattice Boltzmann method should offer the best starting point for the determination of the optimal parameters that has been proposed to date. We will show that such a set exists for our method and that all leading order errors in the diffusion can be removed by the derived set of relaxation rates under appropriate conditions.

The current paper is the first part of a series of two. In this part we give the details on the derivation of the method in a format that should enable the reader to implement our method directly. The numerical section of the paper contains only comparisons to flows with known solution in order to confirm the fourth order convergence. In the second part of the series [24] we apply the method proposed here to simulate flow around a sphere in the Reynolds number range corresponding to the drag crisis in order to demonstrate the fidelity of our method and its relevance for the simulation of real world turbulent fluid mechanics.

2. Cumulant lattice Boltzmann model

In this section we briefly recall the theory of cumulants in the context of the lattice Boltzmann equation.

In the lattice Boltzmann equation we deal with the discrete momentum distribution function $f_{ijkxyzt}$ where the indexes i, j $k \in \mathbb{Z}$ indicate the velocity coordinate in x, y and z direction and t is the discrete time coordinate. Specifically, for a discretization of the lattice Boltzmann equation on a Cartesian lattice using 27 velocities as in [18] we have the set of discrete velocities $i, j, k \in \{-1, 0, 1\}$. This distribution evolves by streaming on a discrete Cartesian grid and by subsequent collision at grid nodes. The collision at grid nodes drives the distribution function closer to equilibrium. In the context of cumulants, equilibrium is usually the state at which all non-conserved cumulants vanish (in practice there are a few exceptions from this rule which will be explained below). The time scale of the collision frequency is made independent of the time step by interpolating or extrapolating between the incoming state and the equilibrium state. When extrapolation is used the physical time between collisions τ can be made arbitrarily shorter than the numerical time step Δt.

The macroscopic transport coefficient (i.e. viscosity) is governed by the time scale τ_1 of binary collisions while the lattice Boltzmann algorithm incorporates also events of higher order. It is desirable to assign different time scales (or equivalently collision rates) to different types of events. This requires us to transform the discrete momentum distribution function into an equivalent set of observable quantities. Since our aim is to assign different rates to different quantities it is essential to choose the quantities such that they are mutually uncorrelated. Correlated quantities would necessarily evolve on the same time scale. Originally, it was proposed to apply a linear transformation of the

distribution function in order to obtain raw moments and assign different rates to them [3, 4]. Unfortunately, as we have shown [18], raw moments are not uncorrelated and assigning different rates to them causes various problems, including break down of Galilean invariance, hyper-viscosity and instability. A better choice is to start from the actual definition of mutual statistical independence and use factorization of the distribution function. Taking the logarithm of the factorized distribution function in Laplace space and taking the series expansion of the result gives the cumulants of the distribution function. The detailed procedure is given in [18]. Cumulants are by design uncorrelated such that it is admissible to assign different relaxation rates to them.

Cumulants, as opposed to moments, might be a rather unfamiliar concept for some readers. It is, however, interesting to note that cumulants play a large role in our perception of the real world. This becomes clear when we consider, as an example, the state of an ideal gas. In terms of velocity moments, we would describe the state of the ideal gas by its extensive quantities such as mass, momentum and energy. Keeping mass as the only extensive quantity we could also describe the gas by its intensive cumulants velocity and temperature. The moments (mass, momentum and energy) contain the same information as the cumulants (mass, velocity and temperature). Which description is more suitable depends on what we are trying to do. For example, conservation laws are more readily stated in terms of moments as these are the actual conserved quantities. Cumulants like velocity and temperature are not conserved. On the other hand, it is no accident that in our daily life we understand the world more readily in terms of the cumulants velocity and temperature. It is these cumulants that initiate fluxes of momentum and energy. Two media in contact will exchange momentum only if they have different velocities and two bodies exchange energy only if they have different temperatures. Inevitably, cumulants determine what is in equilibrium and what is not.

2.1. Relationship of the cumulant LBM to MRT and BGK

Here we briefly address the differences between the classical MRT lattice Boltzmann model from d'Humières [4] which we investigated in detail in [18]. From a practical point of view it is of note that the classical MRT method is mostly applied with lattices having 13, 15 or 19 speeds [25, 26, 4] in three dimensions. We argued based on previous work [27, 28, 29] that 27 speeds is the minimum for the simulation of turbulent flow. In addition, the cumulant lattice Boltzmann method does not apply a Taylor expansion in the equilibrium. The non-linearity is introduced through the non-linear cumulant transform itself. It is the nature of the cumulant ansatz that the equilibrium function is never explicitly given because the equilibrium is defined through the non-conserved cumulants being zero. Expressed in terms of moments this means that higher than second order terms in velocity are present in the equilibrium moments. The cumulant method also includes a small correction in the second order cumulants that compensates for the absence of three third order cumulants as independent quantities. This means the equilibria of second order cumulants are not zero since they have to included the corrections (see equations (34)-(36) below). Due to this correction and the third order terms in velocity in the cumulant transformation, the spurious dependency of the viscosity on the velocity could be eliminated (see Appendix H in [18] for a detailed discussion). However, everything mentioned so far could in principle also be done for the original MRT method, and it has been done in [18] to highlight the real differences between the moment approach of the MRT and our cumulant approach. In both approaches an attempt is made to separate the different degrees of freedom of the distribution. In both cases, q discrete speeds translate into q linearly independent moments or cumulants. Both approaches disagree fundamentally on the concept of mutual independence of the respective observable quantities. The approach used by d'Humières [4] is based on a transformation matrix which is multiplied to a vector of local distributions to obtain a vector of local moments. This matrix is made orthogonal by Gram-Schmidt orthogonalization. To our knowledge, no concise justification for this step has ever been given in literature, but we conjecture that it is meant to make the equivalent partial differential equations of the different moments mutual independent. We like to point out that, if that had been successful, we should expect that the equilibrium of the different moments would be mutually independent, i.e. that the equilibrium of the third order moments would be independent from velocity. In d'Humières' method this is not the case. In [18] we demonstrated by numerical experiments and asymptotic analysis that the orthogonalization of the transformation matrix is the origin of a spurious coupling of the observable quantities on the level of the equivalent partial differential equations (see in particular Appendix I in [18]). This coupling results in a substantial reduction of stability, even compared to a MRT method with non-orthogonal transformation matrix.

In the cumulant method we also aim on mutual independence of the observable quantities. But instead of using an orthogonal matrix, statistical independence is imposed directly by demanding that the momentum distribution function can be written as the product of the distributions of the individual observable quantities. This is the actual definition

of statistical independence, and it is the rationale behind the concept of cumulants in general. Cumulants possess the obvious indicator for mutual independence: unlike in the classical MRT scheme, all equilibria of all cumulants are independent of the conserved quantities (this is, excluding the above mentioned exception of viscosity corrections due to the anisotropy of the lattice). The cumulant method has the same number of independent relaxation rates as a moment based MRT method on the same lattice. Also, symmetry constraints the number of independently tunable parameters. Due to the genuine independence between the cumulants it is found that the relaxation rates of cumulants of order four or higher do not participate in the leading error to the Navier-Stokes equation [18]. This fact will be used in our derivation below. Interestingly, this is a difference between the MRT method and the cumulant method. In the moment based MRT method the relaxation times of fourth order moments have a strong influence on the leading order error. This could both be an advantage or a disadvantage of the MRT, depending on the point of view. We also showed that the moment transformation in the MRT breaks Galilean invariance even for an infinite number of discrete speeds [18] whereas the level of attainable Galilean invariance is only limited by the velocity set in the cumulant method.

It is of note that a different MRT method exists, called the cascaded lattice Boltzmann method, which is based on central moments [30, 31, 32, 33, 34]. The cascaded lattice Boltzmann method has similar properties to the cumulant method in regards of Galilean invariance, but it does not address the subject of mutual independence between the observable quantities. Both the cascaded and the cumulant method select the moment basis with regard to the underlying velocity set whereas the classical MRT method selects the moment basis according to physical considerations. For example, the MRT method typically includes the heat flux as an observable quantity. Dubois et al. [35] recently investigated the difference between the two choices and came to the conclusion that the choice in the d'Humières scheme deteriorates the stability if the transformation is applied in a non-zero velocity reference frame (peculiar or other). The same study finds that the choice of moments made in the cascaded and cumulant method maximizes stability in a non-zero velocity reference frame. Finally, it is of note that the cumulant method and the MRT method behave differently when all relaxation rates are set to the same value. In fact, both the classical MRT method and the central moment method recover the BGK method [36] with an appropriate equilibrium (for the opposite case where the central moment method is forced to recover the second order equilibrium of the standard BGK method see the recent work of De Rosis [37, 38, 39, 40]). The cumulant method differs in that regard due to the fact that the cumulant transformation is not only non-linear in the conserved quantities but also non-linear in the non-conserved quantities. This difference merits its own study and we will not elaborate on it here. We only note that the difference between the single relaxation time cumulant method and the BGK method is extremely small in an asymptotic sense. In diffusive scaling with the smallness parameter ϵ proportional to Knudsen and Mach number, the deviation in the equation of motion of the first cumulant (i.e. the momentum equation) is of $O(\epsilon^4)$ meaning that it is two asymptotic orders smaller than the leading error of the lattice Boltzmann equation. It might therefore be very difficult to actually measure this difference in any actual simulation.

3. The cumulant LBM kernel

In this section we recall the cumulant lattice Boltzmann formulation for the sake of self-containment and for helping the reader to implement our method. This section is largely based on [18]. However, we repeat the equations in full here because we need to introduce a few important changes to our previous method. We note that the collision operator presented here is derived from the one in Appendix J of [18] which is better conditioned than the one in section 4 of [18]. In the current presentation we omit the forcing term and refer the interested reader to the original work. In what follows we will introduce two free parameters A and B which will be determined later.

First, let us recall that the particle distribution function $f_{ijkxyzt}$ is typically considered to be a positive function with the sum over all directions, denoted by ρ, staying close to unity. Such a definition is numerically sub-optimal since it adds a constant offset to all the distributions $f_{ijkxyzt}$ while we are actually only interested in their fluctuations. For this reason, instead of using the distributions directly we store the so-called well conditioned distributions $\mathrm{f}_{ijkxyzt} = f_{ijkxyzt} - \mathrm{w}_{ijk}$, where $\mathrm{w}_{000} = 8/27$, $\mathrm{w}_{100} = 2/27$, $\mathrm{w}_{110} = 1/54$, $\mathrm{w}_{111} = 1/216$ and so on by permuting the indexes.

The density is computed from the zeroth moment $\rho = \delta\rho + 1$ with $\delta\rho = m_{000}$ being the zeroth order raw moment.

Raw moments of the well conditioned pre-collision momentum distribution function are defined as:

$$m_{\alpha\beta\gamma} = \sum_{i=-1}^{1}\sum_{j=-1}^{1}\sum_{k=-1}^{1} i^{\alpha} j^{\beta} k^{\gamma} \mathrm{f}_{ijk}. \tag{1}$$

Here the indexes in space and time are omitted since the collision operator depends only on local quantities. The order of a moment is the sum of its indexes $\alpha+\beta+\gamma$. When evaluating the moments it is always assumed that $0^0 := 1$.

The velocity is computed from the first moments by dividing by the mass:

$$u = \frac{m_{100}}{\rho}, \qquad v = \frac{m_{010}}{\rho}, \qquad w = \frac{m_{001}}{\rho}. \tag{2}$$

3.1. Forward central moment transformation

Since we started from the well conditioned distributions f_{ijk} we have to introduce the constant parameters K that can be computed from the weights w_{ijk}:

$$\mathrm{K}_{ij|\gamma} = \sum_{k} k^{\gamma} \mathrm{w}_{ijk}, \tag{3}$$

$$\mathrm{K}_{i|\beta\gamma} = \sum_{j} j^{\beta} \mathrm{K}_{ij|\gamma}, \tag{4}$$

$$\mathrm{K}_{\alpha\beta\gamma} = \sum_{i} i^{\alpha} \mathrm{K}_{i|\beta\gamma}. \tag{5}$$

These parameters model the global equilibrium at unit mass and zero velocity which has been subtracted from the distributions for better conditioning. However, this subtracted part has to be considered in all non-linear transformations that follow.

Cumulants are efficiently computed from central moments. This is done by the following fast central moment transform

$$\kappa_{ij|0} = (\mathrm{f}_{ij1} + \mathrm{f}_{ij\bar{1}}) + \mathrm{f}_{ij0}, \tag{6}$$

$$\kappa_{ij|1} = (\mathrm{f}_{ij1} - \mathrm{f}_{ij\bar{1}}) - w(\kappa_{ij|0} + \mathrm{K}_{ij|0}), \tag{7}$$

$$\kappa_{ij|2} = (\mathrm{f}_{ij1} + \mathrm{f}_{ij\bar{1}}) - 2w(\mathrm{f}_{ij1} - \mathrm{f}_{ij\bar{1}}) + w^2(\kappa_{ij|0} + \mathrm{K}_{ij|0}), \tag{8}$$

$$\kappa_{i|0\gamma} = (\kappa_{i1|\gamma} + \kappa_{i\bar{1}|\gamma}) + \kappa_{i0|\gamma}, \tag{9}$$

$$\kappa_{i|1\gamma} = (\kappa_{i1|\gamma} - \kappa_{i\bar{1}|\gamma}) - v(\kappa_{i|0\gamma} + \mathrm{K}_{i|0\gamma}), \tag{10}$$

$$\kappa_{i|2\gamma} = (\kappa_{i1|\gamma} + \kappa_{i\bar{1}|\gamma}) - 2v(\kappa_{i1|\gamma} - \kappa_{i\bar{1}|\gamma}) + v^2(\kappa_{i|0\gamma} + \mathrm{K}_{i|0\gamma}), \tag{11}$$

$$\kappa_{0\beta\gamma} = (\kappa_{1|\beta\gamma} + \kappa_{\bar{1}|\beta\gamma}) + \kappa_{0|\beta\gamma}, \tag{12}$$

$$\kappa_{1\beta\gamma} = (\kappa_{1|\beta\gamma} - \kappa_{\bar{1}|\beta\gamma}) - u(\kappa_{0\beta\gamma} + \mathrm{K}_{0\beta\gamma}), \tag{13}$$

$$\kappa_{2\beta\gamma} = (\kappa_{1|\beta\gamma} + \kappa_{\bar{1}|\beta\gamma}) - 2u(\kappa_{1|\beta\gamma} - \kappa_{\bar{1}|\beta\gamma}) + u^2(\kappa_{0\beta\gamma} + \mathrm{K}_{0\beta\gamma}). \tag{14}$$

Throughout this paper we write indexes in Miller notation [41] with $\bar{1} = -1$.

3.2. Forward cumulant transformation

The non-conserved cumulants $c_{\alpha\beta\gamma}$ are computed from the central moments. There is no simple general equation for the computation of cumulants (see [18] for the theory). Since the equilibrium of most cumulants is zero the normalization is omitted in the following and we define:

$$C_{\alpha\beta\gamma} = c_{\alpha\beta\gamma}\rho. \tag{15}$$

In what follows we omit equations for cumulants which can be obtained by permuting indexes in the listed equations. The first few cumulants are seen to be identical to the first few central moments:

$$C_{110} = \kappa_{110}, \tag{16}$$
$$C_{200} = \kappa_{200}, \tag{17}$$
$$C_{120} = \kappa_{120}, \tag{18}$$
$$C_{111} = \kappa_{111}. \tag{19}$$

Equations for C_{101} and C_{011} and so on are obtained by permuting the indexes in the above. Differences from central moments start at order four:

$$C_{211} = \kappa_{211} - ((\kappa_{200} + 1/3)\kappa_{011} + 2\kappa_{110}\kappa_{101})/\rho, \tag{20}$$
$$C_{220} = \kappa_{220} - (((\kappa_{200}\kappa_{020} + 2\kappa_{110}^2) + (\kappa_{200} + \kappa_{020})/3)/\rho - (\delta\rho/\rho)/9), \tag{21}$$
$$C_{122} = \kappa_{122} - ((\kappa_{002}\kappa_{120} + \kappa_{020}\kappa_{102} + 4\kappa_{011}\kappa_{111} + 2(\kappa_{101}\kappa_{021} + \kappa_{110}\kappa_{012})) + (\kappa_{120} + \kappa_{102})/3)/\rho, \tag{22}$$
$$\begin{aligned} C_{222} = {} & \kappa_{222} - (4\kappa_{111}^2 + \kappa_{200}\kappa_{022} + \kappa_{020}\kappa_{202} + \kappa_{002}\kappa_{220} + 4(\kappa_{011}\kappa_{211} + \kappa_{101}\kappa_{121} + \kappa_{110}\kappa_{112}) \\ & +2(\kappa_{120}\kappa_{102} + \kappa_{210}\kappa_{012} + \kappa_{201}\kappa_{021}))/\rho \\ & +(16\kappa_{110}\kappa_{101}\kappa_{011} + 4(\kappa_{101}^2\kappa_{020} + \kappa_{011}^2\kappa_{200} + \kappa_{110}^2\kappa_{002}) + 2\kappa_{200}\kappa_{020}\kappa_{002})/\rho^2 \\ & -(3(\kappa_{022} + \kappa_{202} + \kappa_{220}) + (\kappa_{200} + \kappa_{020} + \kappa_{002}))/(9\rho) \\ & +2(2(\kappa_{101}^2 + \kappa_{011}^2 + \kappa_{110}^2) + (\kappa_{002}\kappa_{020} + \kappa_{002}\kappa_{200} + \kappa_{020}\kappa_{200}) + (\kappa_{002} + \kappa_{020} + \kappa_{200})/3)/(3\rho^2) \\ & +(\delta\rho^2 - \delta\rho)/(27\rho^2), \end{aligned} \tag{23}$$

and so on by permuting indexes.

3.3. Collision

The collision reads explicitly:

$$C_{110}^* = (1 - \omega_1)C_{110}, \tag{24}$$
$$C_{101}^* = (1 - \omega_1)C_{101}, \tag{25}$$
$$C_{011}^* = (1 - \omega_1)C_{011}. \tag{26}$$

The asterisk indicates the post-collison value of any quantity. Due to the anisotropy of the underlying lattice it is necessary to add a few correction terms to the equilibrium. These terms depend on the knowledge of the first order velocity gradients which can be computed from second order cumulants in the following way:

$$D_x u = -\frac{\omega_1}{2\rho}(2C_{200} - C_{020} - C_{002}) - \frac{\omega_2}{2\rho}(C_{200} + C_{020} + C_{002} - \kappa_{000}), \tag{27}$$
$$D_y v = D_x u + \frac{3\omega_1}{2\rho}(C_{200} - C_{020}), \tag{28}$$
$$D_z w = D_x u + \frac{3\omega_1}{2\rho}(C_{200} - C_{002}), \tag{29}$$
$$D_x v + D_y u = -\frac{3\omega_1}{\rho}C_{110}, \tag{30}$$
$$D_x w + D_z u = -\frac{3\omega_1}{\rho}C_{101}, \tag{31}$$
$$D_y w + D_z v = -\frac{3\omega_1}{\rho}C_{011}, \tag{32}$$
$$\tag{33}$$

The following cumulants have non-zero equilibrium due to the mentioned anisotropy of the discretization:

$$C^*_{200} - C^*_{020} = (1-\omega_1)(C_{200} - C_{020}) - 3\rho\left(1 - \frac{\omega_1}{2}\right)(u^2 D_x u - v^2 D_y v), \tag{34}$$

$$C^*_{200} - C^*_{002} = (1-\omega_1)(C_{200} - C_{002}) - 3\rho\left(1 - \frac{\omega_1}{2}\right)(u^2 D_x u - w^2 D_z w), \tag{35}$$

$$C^*_{200} + C^*_{020} + C^*_{002} = \kappa_{000}\omega_2 + (1-\omega_2)(C_{200} + C_{020} + C_{002}) - 3\rho\left(1 - \frac{\omega_2}{2}\right)(u^2 D_x u + v^2 D_y v + w^2 D_z w). \tag{36}$$

It is of note that equations (34) - (36) are part of the original cumulant method. The appearance of the derivatives of velocity in them cancels the spurious dependency of the viscosity on the velocity which is found in many other lattice Boltzmann schemes (see Appendix H of [18] for a detailed discussion and Appendix B in the current paper for a possible modification that also cancels the phase error).

The equilibria for all remaining cumulants are zero in the original cumulant method. Here, however, we introduce new terms in some of the fourth order cumulants:

$$C^*_{120} + C^*_{102} = (1-\omega_3)(C_{120} + C_{102}), \tag{37}$$

$$C^*_{210} + C^*_{012} = (1-\omega_3)(C_{210} + C_{012}), \tag{38}$$

$$C^*_{201} + C^*_{021} = (1-\omega_3)(C_{201} + C_{021}), \tag{39}$$

$$C^*_{120} - C^*_{102} = (1-\omega_4)(C_{120} - C_{102}), \tag{40}$$

$$C^*_{210} - C^*_{012} = (1-\omega_4)(C_{210} - C_{012}), \tag{41}$$

$$C^*_{201} - C^*_{021} = (1-\omega_4)(C_{201} - C_{021}), \tag{42}$$

$$C^*_{111} = (1-\omega_5)C_{111}, \tag{43}$$

$$C^*_{220} - 2C^*_{202} + C^*_{022} = \frac{2}{3}\left(\frac{1}{\omega_1} - \frac{1}{2}\right)\omega_6 A\rho(D_x u - 2D_y v + D_z w) + (1-\omega_6)(C_{220} - 2C_{202} + C_{022}), \tag{44}$$

$$C^*_{220} + C^*_{202} - 2C^*_{022} = \frac{2}{3}\left(\frac{1}{\omega_1} - \frac{1}{2}\right)\omega_6 A\rho(D_x u + D_y v - 2D_z w) + (1-\omega_6)(C_{220} + C_{202} - 2C_{022}), \tag{45}$$

$$C^*_{220} + C^*_{202} + C^*_{022} = -\frac{4}{3}\left(\frac{1}{\omega_1} - \frac{1}{2}\right)\omega_7 A\rho(D_x u + D_y v + D_z w) + (1-\omega_7)(C_{220} + C_{202} + C_{022}), \tag{46}$$

$$C^*_{211} = -\frac{1}{3}\left(\frac{1}{\omega_1} - \frac{1}{2}\right)\omega_8 B\rho(D_y w + D_z v) + (1-\omega_8)C_{211}, \tag{47}$$

$$C^*_{121} = -\frac{1}{3}\left(\frac{1}{\omega_1} - \frac{1}{2}\right)\omega_8 B\rho(D_x w + D_z u) + (1-\omega_8)C_{121}, \tag{48}$$

$$C^*_{112} = -\frac{1}{3}\left(\frac{1}{\omega_1} - \frac{1}{2}\right)\omega_8 B\rho(D_x v + D_y u) + (1-\omega_8)C_{112}, \tag{49}$$

$$C^*_{221} = (1-\omega_9)C_{221}, \tag{50}$$

$$C^*_{212} = (1-\omega_9)C_{212}, \tag{51}$$

$$C^*_{122} = (1-\omega_9)C_{122}, \tag{52}$$

$$C^*_{222} = (1-\omega_{10})C_{222}. \tag{53}$$

The original cumulant LBM is recovered by setting A and B equal to zero. These parameters are introduced to repair some of the errors related to the anisotropy of the lattice. They will be determined later.

3.4. Backward cumulant transformation

After the collision the cumulants have to be transformed back into central moments:

$$\kappa^*_{211} = C^*_{211} + ((\kappa^*_{200} + 1/3)\kappa^*_{011} + 2\kappa^*_{110}\kappa^*_{101})/\rho, \tag{54}$$
$$\kappa^*_{220} = C^*_{220} + (((\kappa^*_{200}\kappa^*_{020} + 2\kappa^{*2}_{110}) + (\kappa^*_{200} + \kappa^*_{020})/3)/\rho - (\delta\rho/\rho)/9), \tag{55}$$
$$\kappa^*_{122} = C^*_{122} + ((\kappa^*_{002}\kappa^*_{120} + \kappa^*_{020}\kappa^*_{102} + 4\kappa^*_{011}\kappa^*_{111} + 2(\kappa^*_{101}\kappa^*_{021} + \kappa^*_{110}\kappa^*_{012})) + (\kappa^*_{120} + \kappa^*_{102})/3)/\rho, \tag{56}$$
$$\begin{aligned}\kappa^*_{222} = {} & C^*_{222} + (4\kappa^{*2}_{111} + \kappa^*_{200}\kappa^*_{022} + \kappa^*_{020}\kappa^*_{202} + \kappa^*_{002}\kappa^*_{220} + 4(\kappa^*_{011}\kappa^*_{211} + \kappa^*_{101}\kappa^*_{121} + \kappa^*_{110}\kappa^*_{112}) \\ & +2(\kappa^*_{120}\kappa^*_{102} + \kappa^*_{210}\kappa^*_{012} + \kappa^*_{201}\kappa^*_{021}))/\rho \\ & -(16\kappa^*_{110}\kappa^*_{101}\kappa^*_{011} + 4(\kappa^{*2}_{101}\kappa^*_{020} + \kappa^{*2}_{011}\kappa^*_{200} + \kappa^{*2}_{110}\kappa^*_{002}) + 2\kappa^*_{200}\kappa^*_{020}\kappa^*_{002})/\rho^2 \\ & +(3(\kappa^*_{022} + \kappa^*_{202} + \kappa^*_{220}) + (\kappa^*_{200} + \kappa^*_{020} + \kappa^*_{002}))/(9\rho) \\ & -2(2(\kappa^{*2}_{101} + \kappa^{*2}_{011} + \kappa^{*2}_{110}) + (\kappa^*_{002}\kappa^*_{020} + \kappa^*_{002}\kappa^*_{200} + \kappa^*_{020}\kappa^*_{200}) + (\kappa^*_{002} + \kappa^*_{020} + \kappa^*_{200})/3)/(3\rho^2) \\ & -(\delta\rho^2 - \delta\rho)/(27\rho^2).\end{aligned} \tag{57}$$

The remaining central moments are obtained by permuting the corresponding indexes. Second and third order central moments are directly obtained from the cumulants according to equations (16)-(19).

3.5. Backward central moment transformation

The back transformation to distributions reads:

$$\kappa^*_{0|\beta\gamma} = \kappa^*_{0\beta\gamma}(1-u^2) - 2u\kappa^*_{1\beta\gamma} - \kappa^*_{2\beta\gamma} - \mathrm{K}_{0\beta\gamma}u^2, \tag{58}$$
$$\kappa^*_{\bar{1}|\beta\gamma} = ((\kappa^*_{0\beta\gamma} + \mathrm{K}_{0\beta\gamma})(u^2-u) + \kappa^*_{1\beta\gamma}(2u-1) + \kappa^*_{2\beta\gamma})/2, \tag{59}$$
$$\kappa^*_{1|\beta\gamma} = ((\kappa^*_{0\beta\gamma} + \mathrm{K}_{0\beta\gamma})(u^2+u) + \kappa^*_{1\beta\gamma}(2u+1) + \kappa^*_{2\beta\gamma})/2, \tag{60}$$
$$\kappa^*_{i0|\gamma} = \kappa^*_{i|0\gamma}(1-v^2) - 2v\kappa^*_{i|1\gamma} - \kappa^*_{i|2\gamma} - \mathrm{K}_{i|0\gamma}v^2, \tag{61}$$
$$\kappa^*_{i\bar{1}|\gamma} = ((\kappa^*_{i|0\gamma} + \mathrm{K}_{i|0\gamma})(v^2-v) + \kappa^*_{i|1\gamma}(2v-1) + \kappa^*_{i|2\gamma})/2, \tag{62}$$
$$\kappa^*_{i1|\gamma} = ((\kappa^*_{i|0\gamma} + \mathrm{K}_{i|0\gamma})(v^2+v) + \kappa^*_{i|1\gamma}(2v+1) + \kappa^*_{i|2\gamma})/2, \tag{63}$$
$$\mathrm{f}^*_{ij0} = \kappa^*_{ij|0}(1-w^2) - 2w\kappa^*_{ij|1} - \kappa^*_{ij|2} - \mathrm{K}_{ij|0}w^2, \tag{64}$$
$$\mathrm{f}^*_{ij\bar{1}} = ((\kappa^*_{ij|0} + \mathrm{K}_{ij|0})(w^2-w) + \kappa^*_{ij|1}(2w-1) + \kappa^*_{ij|2})/2, \tag{65}$$
$$\mathrm{f}^*_{ij1} = ((\kappa^*_{ij|0} + \mathrm{K}_{ij|0})(w^2+w) + \kappa^*_{ij|1}(2w+1) + \kappa^*_{ij|2})/2. \tag{66}$$

4. Parametrization of fourth order cumulants

In the above collision operator we introduced the parameters A and B in the equilibrium of fourth order cumulants. In general the equilibrium of all non-conserved cumulants should be zero. Here we need to take into consideration that the discretization leads to some anisotropy due to missing cumulants. To compensate the anisotropy a non-zero equilibrium might be required. To this end we make a generic ansatz for the equilibrium of the fourth order cumulants. In principle this ansatz could contain all known quantities multiplied with a free parameter each which we determine by asymptotic analysis. It is, however, possible to determine which quantities might appear in the equilibria and which not. First let us note that we are interested in the correction of the leading error only. Asymptotic expansion in diffusive scaling implies that the leading error depends only on the second order in Mach and Knudsen number of the fourth order cumulants. Further we restrict ourselves to terms linear in velocity since we will be focusing on diffusion of momentum in the following. The only terms that fulfill all these constraints (second order, linear in velocity) are the first spatial derivatives of the velocities. Without doing the asymptotic analysis we can exclude most of these derivatives from the equilibria of the fourth order cumulants by simple symmetry arguments. Taking the cumulant C_{211} as an example and investigating its chirality, it is easy to see that C_{211} changes sign under an exchange of the coordinate $z \to -z$ and $w \to -w$ and also under the exchange $y \to -y$ and $v \to -v$. However, it keeps the sign under an exchange $x \to -x$ and $u \to -u$ since the transformation is quadratic in u and x. All terms appearing in the equilibrium

of C_{211} must have the same chirality properties. Now note that $\partial_y w$ and $\partial_z v$ have the same chirality properties as C_{211} and that all other first derivatives of the velocity have different chirality properties which means they cannot appear in the equilibrium of C_{211}. Even the derivative $\partial_x u$ which appears to have the same chirality properties as C_{211} because it keeps sign under $x \to -x$ and $u \to -u$ could in fact be transformed under the assumption of incompressibility, which is valid at second order in diffusive scaling, to $-\partial_y v - \partial_z w$ which does not change sign under either $y \to -y, v \to -v$ and $z \to -z, w \to -w$ and is therefore not a feasible term in the equilibrium of C_{211}. We hence conclude that the equilibrium of C_{211} can only be a function of $\partial_y w$ and $\partial_z v$. For symmetry reasons, the coefficient in front of both derivatives must be the same so that the only feasible modification of the equilibrium of the cumulant C_{211} is found to be:

$$C_{211}^{eq} = \tilde{B}\rho(\partial_y w + \partial_z v). \tag{67}$$

For simplifying the notation during the asymptotic analysis we redefined the parameter without loss of generality to:

$$B = -\frac{1}{3}\left(\frac{1}{\omega_1} - \frac{1}{2}\right)\tilde{B} \tag{68}$$

For symmetry reasons the coefficients in the cumulants C_{121} and C_{112} must be the same. A similar argument leads to the equilibrium for $C_{220} - 2C_{202} + C_{022}$ and $C_{220} + C_{202} - 2C_{022}$. Here again, the coefficient must be the same for symmetry reasons. It is hence seen that there are only two admissible modifications to the equilibrium of the fourth order cumulants that can be used in order to optimize the method by choosing the parameters A and B.

5. Optimal parameter selection

In the cumulant collision kernel ω_1 is chosen to set the shear viscosity and ω_2 is chosen to set the bulk viscosity [4, 43]. All the remaining relaxation rates and the newly introduced parameters A and B do not influence the solution to leading order, yet they influence the error. It is admissible to chose all remaining relaxation rates to be one and A and B to be zero. In fact, this might be the most stable choice, but it is not the most accurate.

The question of how to select the relaxation rates for the ghost quantities is not new. The same problem occurs in the original MRT method and different approaches have been proposed. For example, in the landmark paper on MRT in three dimensions [4] a fixed set of relaxation rates was proposed which was obtained through dispersion analysis. Details of the procedure were not given and all relaxation rates were constant, i.e. independent of viscosity. This is at odds with the theory of "magic" or "quartic" parameters. Ginzburg and Adler found [6] that the solution of the lattice Boltzmann equation were fully controlled by the physical parameters (Reynolds number, Péclet number and so on) once certain "magic" parameters Λ_{oe} were kept constant. It was also shown [1] that the bounce-back and the anti-bounce-back rules kept this property exactly, while some popular interpolation schemes [44] fail to do so [9, 8, 5]. The magic parameters are defined as:

$$\Lambda_{oe} = \left(\frac{1}{\omega_o} - \frac{1}{2}\right)\left(\frac{1}{\omega_e} - \frac{1}{2}\right), \tag{69}$$

where ω_o and ω_e are the relaxation rates of some odd order and even order moments/cumulants, respectively. In order for Λ_{oe} to be constant ω_o should be a function of ω_e. It is hence *a priori* unlikely that there is a single choice of relaxation rates independent of viscosity that fulfills some definition of an optimum. We shall rather assume that the optimal choice for the undetermined relaxation rate will be a function of shear and bulk viscosity, and our task is to determine this relationship.

In the past, the selection of optimal relaxation rates was only partially successful. Early work in the search for suitable magic parameters focused on special cases, such as the accuracy of the position of the wall in Poiseuille flow [6, 9] which was governed by only one relevant combination of odd/even relaxation rates. This justifies to study the magic parameters primarily in the context of the two-relaxation time approximation [8]. It is also found that the parametrization by a single magic parameter is sufficient for Stokes flow [5]. However, it was also found, especially in the context of the advection diffusion equation, that not all errors can be be eliminated by the proper choice of the magic parameter alone [45, 14] and that the most accurate choice of magic parameter is not the most stable one [46].

The improvement of the method by a proper choice of the magic parameter(s) was successful for special cases, but it required different magic parameters depending on the boundary scheme and with this it was also dependent on the orientation of the wall, such that [1] had to conclude that there was no universal "most accurate" choice of the magic parameter.

The MRT method offers more free relaxation rates than the two relaxation time method. However, since the different moments are not uncorrelated it is difficult in the MRT method to utilize the relaxation rates of the ghost moments for anything other than for the minimization of the defects introduced through the correlations between the moments. With its mutually uncorrelated observable quantities, the cumulant LBM should be the best starting point available for parameter optimization and we show below that this is true.

5.1. Objective

Our objective is to minimize the leading order error of the cumulant lattice Boltzmann method. By this we mean the terms appearing at the fifth order of the asymptotic expansion of the lattice Boltzmann equation in diffusive scaling [47]. In the optimal case, if all error terms could be eliminated simultaneously, the accuracy of the LBM would go from second to fourth order in diffusive scaling. However, this will not be possible by choosing specific relaxation rates alone since there are certain error terms related to violations of Galilean invariance and to finite compressibility that are independent of the relaxation rates. However, all errors related to diffusion (such as hyper-viscosity) are functions of the relaxation rates. It is hence our aim to select the relaxation rates such that spurious diffusion terms vanish from the fifth order of the asymptotic expansion of the lattice Boltzmann equation. In order to do this we should first compute the equivalent partial differential equation for the leading order error of the cumulant lattice Boltzmann equation [47, 48]. That would be quite involved. Since we decided to focus on the diffusion terms we can solve a slightly simpler problem. The errors we are interested in are linear in velocity. Therefore, we linearized the cumulant lattice Boltzmann equation and we will use only Taylor expansion to determine the leading order errors.

5.2. Taylor expansion of the cumulant lattice Boltzmann equation

The lattice Boltzmann equation is conveniently written as

$$f^{*}_{ijk(x+ic\Delta t/2)(y+jc\Delta t/2)(z+kc\Delta t/2)(t+\Delta t/2)} - f_{ijk(x-ic\Delta t/2)(y-jc\Delta t/2)(z-kc\Delta t/2)(t-\Delta t/2)} = 0. \tag{70}$$

With the lattice speed $c = \Delta x/\Delta t$. To eliminate the pre- and post-collision states and in order to introduce the collision operator in distribution form $\Omega^{\mathrm{f}}_{ijkxyzt}$ we define [49, 50]:

$$\begin{aligned} f_{ijkxyzt} &= \bar{f}_{ijkxyzt} - \Omega^{\mathrm{f}}_{ijkxyzt}/2, & (71)\\ f^{*}_{ijkxyzt} &= \bar{f}_{ijkxyzt} + \Omega^{\mathrm{f}}_{ijkxyzt}/2. & (72) \end{aligned}$$

With this equation (70) becomes:

$$\begin{aligned} 0 = {} & \bar{f}_{ijk(x+ic\Delta t/2)(y+jc\Delta t/2)(z+kc\Delta t/2)(t+\Delta t/2)} - \bar{f}_{ijk(x-ic\Delta t/2)(y-jc\Delta t/2)(z-kc\Delta t/2)(t-\Delta t/2)} \\ & + \Omega^{\mathrm{f}}_{ijk(x+ic\Delta t/2)(y+jc\Delta t/2)(z+kc\Delta t/2)(t+\Delta t/2)}/2 + \Omega^{\mathrm{f}}_{ijk(x-ic\Delta t/2)(y-jc\Delta t/2)(z-kc\Delta t/2)(t-\Delta t/2)}/2. \end{aligned} \tag{73}$$

The Taylor expansion of equation (73) is seen to have the nice property that the distributions vanish at all even orders and the collision operator vanishes at all odd orders of the expansion coefficient:

$$0 = \sum_{m,n,o,q=0}^{\infty} \frac{\partial_x^m \partial_y^n \partial_z^o \partial_t^q}{m!n!o!q!} \left(\left(\frac{\Delta t}{2}\right)^{m+n+o+q} c^{m+n+o} i^m j^n k^o\right) \left(\bar{f}_{ijkxyzt}\left(1-(-1)^{m+n+o+q}\right) + \frac{\Omega^{\mathrm{f}}_{ijkxyzt}}{2}\left(1+(-1)^{m+n+o+q}\right)\right). \tag{74}$$

We define the countable raw moments omitting the time and space variables from here on:

$$\bar{m}_{\alpha\beta\gamma} = \sum_{i,j,k} (ic)^{\alpha} (jc)^{\beta} (kc)^{\gamma} \bar{f}_{ijk}. \tag{75}$$

We can hence rewrite (74) by substituting the distributions by (75) and by using the collision operator in moment form $\Omega^{\mathrm{m}}_{ijkxyzt}$:

$$0 = \sum_{m,n,o,q=0}^{\infty} \frac{\partial_x^m \partial_y^n \partial_z^o \partial_t^q}{m!n!o!q!} \left(\frac{\Delta t}{2}\right)^{m+n+o+q} \left(\bar{m}_{(\alpha+m)(\beta+n)(\gamma+o)} \left(1-(-1)^{m+n+o+q}\right) + \frac{\Omega^{\mathrm{m}}_{(\alpha+m)(\beta+n)(\gamma+o)}}{2} \left(1+(-1)^{m+n+o+q}\right) \right). \quad (76)$$

This can be solved for the collision operator:

$$\Omega^{\mathrm{m}}_{\alpha\beta\gamma} = - \sum_{\substack{m,n,o,q=0 \\ m+n+o+q\neq 0}}^{\infty} \frac{\partial_x^m \partial_y^n \partial_z^o \partial_t^q}{m!n!o!q!} \left(\frac{\Delta t}{2}\right)^{m+n+o+q} \left(\bar{m}_{(\alpha+m)(\beta+n)(\gamma+o)} \left(1-(-1)^{m+n+o+q}\right) + \frac{\Omega^{\mathrm{m}}_{(\alpha+m)(\beta+n)(\gamma+o)}}{2} \left(1+(-1)^{m+n+o+q}\right) \right). \quad (77)$$

Equation (77) is a recursive equation. It is used to express the moments through their equilibrium moments in a similar way as proposed by Holdych et al. [51]. In asymptotic analysis we are only interested in a final sum up to a certain power of Δt. For any finite power of Δt we can successively insert (77) into itself to eliminate the dependence of the collision operator from itself. Any final approximation of $\Omega^{\mathrm{m}}_{\alpha\beta\gamma}$ is therefore a function of the moments alone.

The bared moments $\bar{m}_{\alpha\beta\gamma}$ do not actually exist in the simulation but they are obtained from the pre-collision moment $m_{\alpha\beta\gamma}$ and the post-collision moments $m^*_{\alpha\beta\gamma}$:

$$\bar{m}_{\alpha\beta\gamma} = m_{\alpha\beta\gamma} + \Omega^{\mathrm{m}}_{\alpha\beta\gamma}/2, \quad (78)$$

$$\bar{m}_{\alpha\beta\gamma} = m^*_{\alpha\beta\gamma} - \Omega^{\mathrm{m}}_{\alpha\beta\gamma}/2. \quad (79)$$

While the number of countable raw moments is in general infinite, due to the finite number of distributions, our D3Q27 model has only 27 independent moments. Moments with either index (α, β or γ) being larger than two are identical with lower order moments such that $m_{300} = m_{100}$, $m_{040} = m_{020}$ and so on.

The actual collision in our model happens in cumulant space. The relationship between the distributions f and the cumulants is not linear, hence Taylor expansion in space and time cannot be used on cumulants directly. Instead we express the cumulants in the collision operator in terms of raw moments. The collision for any non-conserved cumulant $\bar{C}_\star$ can be expressed using the collision operator in cumulant space $\Omega^{\mathrm{c}}_\star$:

$$\bar{C}_\star = C^{eq}_\star - \tau_\star \Omega^{\mathrm{c}}_\star, \quad (80)$$

where $\tau_\star$ is the relaxation time of the cumulant which is related to the modified relaxation rate via Hénon-correction [52] or Strang-splitting [50]:

$$\tau_\star = \left(\frac{1}{\omega_\star} - \frac{1}{2}\right). \quad (81)$$

As we restricted ourselves to diffusion, which is linear, we can simplify the cumulant transformation significantly by linearizing it around equilibrium. Equilibrium, by definition, is the state at which all non-conserved cumulants are zero. Further we disregard all terms of cubic and higher order in velocity u, v and w. To streamline the notation we assume $\tau_6 = \tau_7 = \tau_h$, since keeping τ_6 and τ_7 independent would inflate our result while these relaxation times are found to be irrelevant at the considered order. None of the above assumptions are necessary. They are used only for streamlining our notation under the assumption that we focus on diffusion (those are not good assumptions if we would consider advection instead). Under the above assumptions the raw moments up to fourth order can be written (omitting cases that can be obtained by permuting indexes; further details on the derivations are found in Appendix A):

$$\bar{m}_{000} = \rho, \tag{82}$$
$$\bar{m}_{100} = u\rho, \tag{83}$$
$$\bar{m}_{010} = v\rho, \tag{84}$$
$$\bar{m}_{002} = w\rho, \tag{85}$$
$$\bar{m}_{200} = \frac{\rho}{3} + u^2\rho - \frac{1}{3}\left((\tau_2 + 2\tau_1)\Omega^{\mathrm{m}}_{200} + (\tau_2 - \tau_1)(\Omega^{\mathrm{m}}_{020} + \Omega^{\mathrm{m}}_{002})\right), \tag{86}$$
$$\bar{m}_{110} = uv\rho - \tau_1\Omega^{\mathrm{m}}_{110}, \tag{87}$$
$$\bar{m}_{102} = \frac{\rho}{3}u - \frac{1}{2}\left((\tau_4 + \tau_3)\Omega^{\mathrm{m}}_{102} + (\tau_4 - \tau_3)\Omega^{\mathrm{m}}_{120}\right), \tag{88}$$
$$\bar{m}_{111} = -\tau_5\Omega^{\mathrm{m}}_{111}, \tag{89}$$
$$\bar{m}_{220} = \rho\frac{1 + 3u^2 + 3v^2}{9} - \frac{2\tau_1 - 2\tau_2}{9}\Omega^{\mathrm{m}}_{002} - \frac{2\tau_2 + \tau_1 - 3\tau_h}{9}(\Omega^{\mathrm{m}}_{200} + \Omega^{\mathrm{m}}_{020}) - \frac{A\tau_1}{3}(\Omega^{\mathrm{m}}_{200} + \Omega^{\mathrm{m}}_{200} - 2\Omega^{\mathrm{m}}_{002}) - \tau_h\Omega^{\mathrm{m}}_{220}, \tag{90}$$
$$\bar{m}_{211} = \frac{\rho}{3}vw - \frac{\tau_1 - \tau_8}{3}\Omega^{\mathrm{m}}_{011} - B\tau_1\Omega^{\mathrm{m}}_{011} - \tau_8\Omega^{\mathrm{m}}_{211}. \tag{91}$$

Moments of order five and higher do not appear in the expansion to the required order and are therefore omitted. Recursively inserting (82) - (91) into (77) and (77) into (82) - (91) until a desired order we can obtain sufficiently accurate approximations of the equivalent partial differential equations of the lattice Boltzmann equation. For example, if we expand only to first order in Δt the mass equation:

$$\Omega^{\mathrm{m}}_{000} = 0, \tag{92}$$

we obtain the continuity equation of an incompressible fluid:

$$\partial_x u\rho + \partial_y v\rho + \partial_z w\rho = O(\Delta t). \tag{93}$$

With a more refined analysis (not shown) we would find that the density ρ can be eliminated from (93).

By expanding the collision operator for the first moment in x direction $\Omega^{\mathrm{m}}_{100} = 0$ up to $O(\Delta t^2)$ and making use of (93) we arrive at the Navier-Stokes equation:

$$\partial_t u\rho = -\partial_x\rho/3 - \partial_x\rho u^2 - \partial_y\rho uv - \partial_z\rho uw + \tau_1/3\rho(\partial_{xx}u + \partial_{yy}u + \partial_{zz}u) + O(\Delta t^2). \tag{94}$$

In order to compute the leading error we evaluate $\Omega^{\mathrm{m}}_{100} = 0$ up to $O(\Delta t^4)$. In this expansion there are still mixed derivatives of velocity in space and time. Wherever such a mixed derivative appears, the time derivative is substituted by the Navier-Stokes equation in moment form, i.e. by:

$$\partial_t\bar{m}_{100} = -\partial_x\bar{m}_{200} - \partial_y\bar{m}_{110} - \partial_z\bar{m}_{101} + O(\Delta t^2), \tag{95}$$
$$\partial_t\bar{m}_{010} = -\partial_x\bar{m}_{110} - \partial_y\bar{m}_{020} - \partial_z\bar{m}_{011} + O(\Delta t^2), \tag{96}$$
$$\partial_t\bar{m}_{001} = -\partial_x\bar{m}_{101} - \partial_y\bar{m}_{011} - \partial_z\bar{m}_{002} + O(\Delta t^2), \tag{97}$$

with the non-conserved moments $\bar{m}_{200}$, $\bar{m}_{110}$ expressed through (86) and (87), respectively. This will eliminate all mixed time/space derivatives of velocity from the leading error.

All the steps outlined here are implemented in a computer algebra system. For disregarding the error in advection we will also drop all terms quadratic in velocity u, v and w. That means we linearize the expanded lattice Boltzmann equation around velocity zero and extract all terms at the leading error proportional to $O(\Delta t^4)$. This gives us the linearized leading error of the lattice Boltzmann momentum equation *LLE*. Since there are three momentum equations

(in x, y and z directions), we consider without loss of generality the linearized leading error in x direction (LLE_x). The linearized leading error can be further simplified by taking equation (93) into account which implies for the fourth order derivatives the following substitutions:

$$\begin{aligned}
\partial_{xzzz}\bar{m}_{001} &= -\partial_{xxzz}\bar{m}_{100} - \partial_{xyzz}\bar{m}_{010}, && (98)\\
\partial_{xyyy}\bar{m}_{010} &= -\partial_{xxyy}\bar{m}_{100} - \partial_{xyyz}\bar{m}_{001}, && (99)\\
\partial_{xxxz}\bar{m}_{001} &= -\partial_{xxxx}\bar{m}_{100} - \partial_{xxxy}\bar{m}_{010}. && (100)
\end{aligned}$$

The linearized leading error hence becomes:

$$\begin{aligned}
LLE_x = &\left[\frac{\tau_1}{36} - \frac{(\tau_3+\tau_4)\tau_1^2}{9} - \frac{(\tau_3-\tau_4)B\tau_1^2}{6} + \frac{\tau_1^3}{9}\right](\partial_{zzzz}u + \partial_{yyyy}u) + \\
&\left[\frac{\tau_1}{18} + \frac{B\tau_1}{6} - \frac{2(\tau_3-\tau_4)\tau_1^2}{9} - \frac{B(\tau_3+\tau_4)\tau_1^2}{3} - \frac{(4+12B)\tau_5\tau_1^2}{9} + \frac{2\tau_1^3}{9}\right]\partial_{yyzz}u + \\
&\frac{1}{108}[2\tau_2(1+12(A-B-1)\tau_3\tau_1) + \tau_1(27B-18A-2+12\tau_1(4\tau_3(A-B-1) + \\
&\tau_4(10+12A-9B) - 4\tau_5(1+3B)))](\partial_{xyzz}v + \partial_{xyyz}w) + \\
&\frac{1}{54}[\tau_2(1+12(A-B-1)\tau_3\tau_1) + \tau_1(2+3(2A+B)\tau_3\tau_1 - 3(4+6A-3B)\tau_4\tau_1)](\partial_{xxyy}u + \partial_{xxzz}u) + \\
&\frac{1}{108}[2\tau_2(12\tau_1\tau_3(1-A+B)-1) + \tau_1(12\tau_1(\tau_3(2A+B) + \tau_4(2-3B)) - 7) + 12\tau_1^3]\partial_{xxxx}u. \qquad (101)
\end{aligned}$$

The last remaining possibility to simplify this result is by recognizing that the relaxation time for the second order cumulants τ_1 is proportional to the viscosity and that we are interested in the domain of small viscosities. Terms proportional to τ_1^3 are numerically small and they are neglected from here on. Apart from that no further simplification can be made.

Before we solve the system for the optimal parameters we mention some observations: The linearized leading error can be split into five independent error terms, each proportional to a different spurious fourth order derivative of velocity and each having a pre-factor which is a function of the relaxation rates for the cumulants. These functions are linearly independent and they form the system:

$$\begin{aligned}
0 &= \tau_1 - 4(\tau_3+\tau_4)\tau_1^2 - 6(\tau_3-\tau_4)B\tau_1^2, && (102)\\
0 &= \tau_1 + 3B\tau_1 - 4(\tau_3-\tau_4)\tau_1^2 - 6B(\tau_3+\tau_4)\tau_1^2 - (8+24B)\tau_5\tau_1^2, && (103)\\
0 &= 2\tau_2(1+12(A-B-1)\tau_3\tau_1) + \tau_1(27B-18A-2+12\tau_1(4\tau_3(A-B-1) + \\
&\quad \tau_4(10+12A-9B) - 4\tau_5(1+3B))), && (104)\\
0 &= \tau_2(1+12(A-B-1)\tau_3\tau_1) + \tau_1(2+3(2A+B)\tau_3\tau_1 - 3(4+6A-3B)\tau_4\tau_1), && (105)\\
0 &= 2\tau_2(12\tau_1\tau_3(1-A+B)-1) + \tau_1(12\tau_1(\tau_3(2A+B) + \tau_4(2-3B)) - 7). && (106)
\end{aligned}$$

While there are ten different relaxation rates in our model, only five appear here, namely two for second order cumulants and three for third order cumulants. The relaxation rates for fourth, fifth and sixth order cumulants do not influence the linearized leading error. The two relaxation times for the second order cumulants τ_1 and τ_2 govern the shear and the bulk viscosity, respectively. They are physical parameters and they must be chosen to fit the parameters of the fluid, they are hence no degrees of freedom for the optimization of the model. Therefore, there are only three relaxation times left to choose. The choice of these rates can be said to be optimal if the linearized leading error for small viscosities vanishes. However, this is hardly possible since there are only three parameters and five independent equations that need to be zero simultaneously. In the original proposal [1] the situation is even more unfavorable since in the two relaxation time model $\tau_3 = \tau_4 = \tau_5$ such that only one parameter could be chosen. Such a choice would

in any case be a compromise and its quality would depend heavily on the flow conditions under consideration (i.e. it would depend on which of the derivatives are small in the given setup).

While there are not enough relaxation times in the regular lattice Boltzmann scheme we observe that the artificially introduced parameters A and B appear in the equations. Including them as the two missing degrees of freedom in the optimization problem we are indeed able to eliminate all terms in the linearized leading error for small viscosity and obtain the following relationships:

$$\tau_3 = \frac{2\tau_2 + \tau_1}{8\tau_1(5\tau_2 + \tau_1)}, \tag{107}$$

$$\tau_4 = \frac{2\tau_2 - 5\tau_1}{8\tau_1(\tau_2 - 7\tau_1)}, \tag{108}$$

$$\tau_5 = \frac{8\tau_2^2 + 17\tau_2\tau_1 + 2\tau_1^2}{24\tau_1(2\tau_2^2 + 9\tau_2\tau_1 + \tau_1^2)}, \tag{109}$$

$$A = -\frac{2(\tau_2^2 - 3\tau_2\tau_1 - \tau_1^2)}{4\tau_2^2 - 5\tau_2\tau_1 + \tau_1^2}, \tag{110}$$

$$B = \frac{2(\tau_2^2 + 16\tau_2\tau_1 + \tau_1^2)}{3(4\tau_2^2 - 5\tau_2\tau_1 + \tau_1^2)}. \tag{111}$$

Which can also be expressed in terms of relaxation rates:

$$\omega_3 = \frac{8(\omega_1 - 2)(\omega_2(3\omega_1 - 1) - 5\omega_1)}{8(5 - 2\omega_1)\omega_1 + \omega_2(8 + \omega_1(9\omega_1 - 26))}, \tag{112}$$

$$\omega_4 = \frac{8(\omega_1 - 2)(\omega_1 + \omega_2(3\omega_1 - 7))}{\omega_2(56 - 42\omega_1 + 9\omega_1^2) - 8\omega_1}, \tag{113}$$

$$\omega_5 = \frac{24(\omega_1 - 2)(4\omega_1^2 + \omega_1\omega_2(18 - 13\omega_1) + \omega_2^2(2 + \omega_1(6\omega_1 - 11)))}{16\omega_1^2(\omega_1 - 6) - 2\omega_1\omega_2(216 + 5\omega_1(9\omega_1 - 46)) + \omega_2^2(\omega_1(3\omega_1 - 10)(15\omega_1 - 28) - 48)}, \tag{114}$$

$$A = \frac{4\omega_1^2 + 2\omega_1\omega_2(\omega_1 - 6) + \omega_2^2(\omega_1(10 - 3\omega_1) - 4)}{(\omega_1 - \omega_2)(\omega_2(2 + 3\omega_1) - 8\omega_1)}, \tag{115}$$

$$B = \frac{4\omega_1\omega_2(9\omega_1 - 16) - 4\omega_1^2 - 2\omega_2^2(2 + 9\omega_1(\omega_1 - 2))}{3(\omega_1 - \omega_2)(\omega_2(2 + 3\omega_1) - 8\omega_1)}. \tag{116}$$

The existence of such a general solution is surprising as it implies that we can solve the diffusion problem to fourth order accuracy on a stencil that accesses only nearest neighbors. According to common wisdom this should be impossible. Having a closer look at our result we see that the solution is not completely general. No solution exists for $\omega_1 = \omega_2$. This is not a big problem since in most cases the bulk viscosity is set larger then the shear viscosity. However, there are other problems: The solution has singularities and ω_4 is not always in the range admissible for linear stability which is the open set from zero to two. However, we observe that there is a reasonable large window of admissible relaxation rates. If we limit us to the case $\omega_2 = 1$, for example, the only critical problems are two singularities of A and B at $\omega_1 = 1$ and $\omega_1 = 2/5$ and that ω_4 becomes negative for $\omega_1 < 7/4$. The operational window is hence $7/4 < \omega_1 < 2$ which covers the open range of viscosity $\left(0 \cdots \frac{1}{42}\frac{\Delta x^2}{\Delta t}\right)$. This is exactly the range of low viscosities which has the highest technical relevance for us, bounded by the inverse of a particular number [42].

It is a noteworthy observation that $\omega_4 \neq \omega_5$ and that $A \neq B$. The relaxation rate ω_4 acts on the cumulants $C_{210} - C_{201}$ and permutations while ω_5 acts on C_{111}. However, these two cumulants can be mapped onto each other by a rotation of the coordinate system. The same goes for the fourth order cumulants $C_{220} - C_{202}$ and C_{211} in which A and B appear. We would usually expect that two cumulants that can be mapped on each other by a rotation of the coordinate system should behave exactly in the same way. The reason why this is not so in the current case is of course that due to the finite number of speeds the equivalent partial differential equations at the order of the leading

error are no longer isotropic. To compensate for this, the corrections must be equally anisotropic, which explains this apparent inconsistency.

We also checked whether we could use a steady state expansion to obtain a sufficient approximation of the optimal parameters for small enough viscosity. The procedure is outlined in Appendix D. The result is negative and so it confirms the importance of considering the transient nature of the Navier-Stokes equation.

5.3. Accuracy of the advection

In this paper we focus on improving the accuracy of the lattice Boltzmann method with regard to diffusion. At the same time there are error terms related to the finite compressibility and errors related to advection. Errors in advection result from the fact that a model that relies on a fixed velocity set cannot be completely Galilean invariant. Compared to most previous lattice Boltzmann methods, the cumulant method [18] improved the Galilean invariance considerably. There is no leading order dependency of the viscosity on the velocity and the advection of a simple shear wave has been demonstrated to be fourth order accurate [18]. A particular advantage of the cumulant method is that the level of Galilean invariance at the order of the leading error is independent from the choice of the relaxation rates, a property not shared by the original MRT method [18]. This is particularly important for the current study as it implies that, even though we did not address Galilean invariance in the derivation of the optimal relaxation rates, we know *a priori* that they will not affect the Galilean invariance at the leading order of the error. Still it might be argued that attaining high accuracy in diffusion is not useful if it is not matched by a similar advance in advection. The good news is that the remaining leading order error in advection can be precisely attributed to three unknown second derivative in velocity $\partial_{xx}u$, $\partial_{yy}v$ and $\partial_{zz}w$. The analysis is given in [53] and the result is shown in Appendix B. Even though this is not the focus of the current paper, we note that a lattice Boltzmann scheme can be implemented that is both fourth order accurate in diffusion and in advection if the missing terms are obtained from finite differences. We will refer to this model as D3Q27F3 model.

5.4. 3D versus 2D

In the field of lattice Boltzmann modeling it is very common to derive a new method first in one or two dimensions followed by an attempt to generalize the result to the three dimensional case. We criticized this practice before [18]. In particular, in the derivation of the cumulant method in two dimensions there is no difference between the cumulant and the central moment method (also called the cascaded method [30]) whereas the error norm of the cumulant method in three dimensions can be four orders of magnitude smaller than the error norm of the central moment method in three dimensions [18]. The reason for this drastic difference is the discrepancy between the behavior of fourth order cumulants in two and three dimensions. In the case of the parametrization for fourth order accurate diffusion, the difference between two and three dimensions is even more drastic. Naively thinking we should expect that it was easier to enforce fourth order accuracy in two dimensions than in three dimensions. Interestingly the opposite is true. The method outlined in this paper cannot be applied to eliminate the *LLE* in two dimensions. A detailed discussion of the *LLE* of the D2Q9 lattice is given in Appendix C.

6. Limiter

The cumulant lattice Boltzmann method with $\omega_3 = \omega_4 = \omega_5 = 1.0$ has excellent stability properties, especially in the limit of very small viscosities. Setting the relaxation rates to one means that the memory of the respective cumulants is erased in every time step. In the case of the optimized parameter set the simulation relies on that memory and therefore it cannot be erased. In fact, for small viscosities at $\omega_1 \to 2$ we have $\omega_3 \to 0$, $\omega_4 \to 0$ and $\omega_5 \to 0$, meaning that these cumulants return very slowly to equilibrium. This might become a problem when the viscosity is too small. Therefore we propose a limiter for the third order cumulants. The purpose of the limiter is to keep the third order cumulants from growing indefinitely without interfering with the fourth order accuracy of the diffusion. This can be done by replacing the relaxation rate ω_3 by $\omega_{120+102}$ which we define as:

$$\omega_{120+102} = \omega_3 + \frac{(1-\omega_3)|C_{120}+C_{102}|}{\rho\lambda_3 + |C_{120}+C_{102}|}. \tag{117}$$

Here λ_3 is the adjustable threshold of the limiter. If $|C_{120} + C_{102}| << \lambda_3\rho$ the limiter has no effect and the optimal rate is used. If $|C_{120} + C_{102}| >> \lambda_3\rho$ the relaxation rate is restored to the stable value of one and the memory of the cumulant is erased. In between the two extremes the relaxation rate approaches the stable value when the cumulant becomes large. According to their asymptotics, all third order cumulants should be third order in diffusive scaling such that $\omega_{120+102} = \omega_3 + O(\epsilon^3)$ with $\Delta t \propto \epsilon^2$ and $\Delta x \propto \epsilon$. The error introduced by the limiter is hence seen to be small in comparison to the linearized leading error of the lattice Boltzmann momentum equation. The fourth order convergence of the diffusion is hence not affected by the choice of λ_3. The same is done for ω_4 and ω_5 using λ_4 and λ_5. The collision operator for the respective cumulants is changed to the limited collision operator:

$$
\begin{aligned}
C^*_{120} + C^*_{102} &= (1 - \omega_{120+102})(C_{120} + C_{102}), && (118)\\
C^*_{210} + C^*_{012} &= (1 - \omega_{210+012})(C_{210} + C_{012}), && (119)\\
C^*_{201} + C^*_{021} &= (1 - \omega_{201+021})(C_{201} + C_{021}), && (120)\\
C^*_{120} - C^*_{102} &= (1 - \omega_{120-102})(C_{120} - C_{102}), && (121)\\
C^*_{210} - C^*_{012} &= (1 - \omega_{210-012})(C_{210} - C_{012}), && (122)\\
C^*_{201} - C^*_{021} &= (1 - \omega_{201-021})(C_{201} - C_{021}), && (123)\\
C^*_{111} &= (1 - \omega_{111})C_{111}, && (124)
\end{aligned}
$$

with the relaxation rates being the limited rates according to (117) with the respective cumulants. Limiting the relaxation rates is optional but it improves stability for very small viscosity.

7. Numerical evaluation

In order to confirm that the optimized parameters improve the diffusion terms to be fourth order accurate we conduct two simple convergence studies: the decay of a double shear wave under constant advection and the decay of an anisotropic Taylor-Green vortex under constant advection, both under diffusive scaling. The tests are the same as presented in [18] for various lattice Boltzmann models. We compare the results to results from four different lattice Boltzmann models: the original cumulant method where $\omega_3 = \omega_4 = \omega_5 = 1$ and $A = B = 0$ (AllOne), the standard BGK model with second order Taylor-expanded equilibrium [54] (BGK), and the BGK model derived from the cumulant lattice Boltzmann model, i.e. Appendix A in [18] (BGK+) and the cumulant lattice Boltzmann model with optimal parametrization and an additional correction of the advection by finite differences according to Appendix B (D3Q27F3). All models are implemented in the well-conditioned form. For the optimized method we compare two thresholds for the limiter, $\lambda_{low} = 0.01$ ($\mathrm{NC}_{0.01}$) and $\lambda_\infty = 10^6$ ($\mathrm{NC}_{1\mathrm{Mio}}$) with the same value applied to all cumulants ($\lambda_3 = \lambda_4 = \lambda_5$). Note that in the case of λ_∞ the limiter is effectively turned off. All models are implemented using 27 discrete velocities (D3Q27 lattice) and double precision.

7.1. Double shear wave decay

We study the decay of a double shear wave in a domain of size $L\times3\Delta x\times3/2L$ with the following initial conditions:

$$
\begin{aligned}
u(t=0) &= u_0 L_0/L, && (125)\\
v(t=0) &= v_0 L_0/L \sin(2\pi x/L)\cos(4\pi z/(3L)), && (126)\\
w(t=0) &= 0. && (127)
\end{aligned}
$$

The analytical solution for this problem is:

$$
\begin{aligned}
u(t) &= u_0 L_0/L, && (128)\\
v(t) &= v_0 L_0/L \sin(2\pi(x+u_0 t)/L)\cos(4\pi z/(3L)) e^{-\nu t\left(\left(\frac{2\pi}{L}\right)^2+\left(\frac{4\pi}{3L}\right)^2\right)}, && (129)\\
w(t) &= 0. && (130)
\end{aligned}
$$

We are interested in the asymptotic behavior of the decay rate of the wave which we measure by varying L from $32\Delta x$ to $512\Delta x$ with $L_0 = 32\Delta x$, $u_0 = 0.096\Delta x/\Delta t$ and $v_0 = 0.1\Delta x/\Delta t$. Each simulation is run for $20000(L/L_0)^2$ time steps and a spatial Fourier transform of $v(t)$ is performed every $1000(L/L_0)^2$ time steps starting at time step $11000(L/L_0)^2$. The decay of the logarithm of the amplitude of the wave is fitted to a linear function to determine the viscosity. Note that the setup is identical to the one used in [18]. The results for four different viscosities $\{10^{-2}, 10^{-3}, 10^{-4}, 10^{-5}\}\Delta x^2/\Delta t$ is depicted in Fig. 1. It is seen that the limiter affects the result only in the case of low viscosity and short wave length. This is to be expected as the limiter has been designed to be asymptotically small compared to the leading error. Still applying a low threshold reduces the accuracy of the result. At the same time, a low threshold of the limiter improves stability. In the case of $L = 32\Delta x$ and $\nu = 10^{-5}\Delta x^2/\Delta t$ the simulation with λ_∞ crashed, implying that the optimized method is less stable than AllOne. Stability is effectively recovered by applying the limiter with λ_{low}.

As for the convergence order, for the two cases with the lower viscosity ($10^{-4}\Delta x^2/\Delta t$ and $10^{-5}\Delta x^2/\Delta t$) a convergence of order 4 is apparent while AllOne obtains only second order convergence. On the other hand, for the higher viscosities ($10^{-2}\Delta x^2/\Delta t$ and $10^{-3}\Delta x^2/\Delta t$) fourth order convergence is not obtained with the optimized relaxation rates. In particular for the highest tested viscosity the convergence order is only quadratic. This might be attributed to the fact that we neglected terms proportional to ν^3 in the linearized leading error. These terms are only small in an absolute sense not in an asymptotic sense such that they will dominate the error at sufficient refinement. It can hence be said that by neglecting these terms from the linearized leading error our solution cannot be regarded as fourth order accurate in a strict sense. However, from a practical engineering point of view this small residual error should be almost irrelevant. In the case of the lower viscosities the residual errors are no longer measurable even with a wavelength of $512\Delta x$. In the case of the highest viscosity, even though the results are clearly second order, the error is more than two orders of magnitude smaller than in the AllOne case and also two orders of magnitude smaller than the errors of the BGK+ method. Compared to the standard BGK method the optimized cumulant method is even three orders of magnitude more accurate in this example. It is of note that the high viscosity case has $\nu = 0.01\Delta x^2/\Delta t$, which is about half the value of the strict upper limit $\nu_{max} = 1/42\Delta x^2/\Delta t \approx 0.0238\Delta x^2/\Delta t$ at which the method becomes unconditionally unstable. While the optimized method is not fourth order accurate so close to its stability limit it still compares most favorable to the other models.

It is also seen that for low enough viscosities and short enough waves length, the optimized parameter set can give slightly inferior results compared to the AllOne and the BGK/BGK+ case. This can be attributed to Runge's phenomenon: increasing the numerical order without increasing the resolution does not necessarily reduces the error. In our case the increase of the error at low resolution is fortunately relatively small.

Fig. 2 shows the phase error acquired when the wave travels three times its own wavelength. This is to investigate the Galilean invariance of our model. We recall that the advection correction is ineffective for a simple traveling shear wave as the corresponding derivatives are always null. It is therefore not surprising that the D3Q27F3 method with advection correction shows no improvement over the uncorrected version in this test. Also, as expected, we do not observe any leading order influence of the optimized parameters on the phase delay. In fact all models appear to be fourth order accurate, with the standard BGK method showing a deviation for larger wavelength. Interestingly, the parameters that we optimized for better diffusion also seem to improve the phase under some conditions. Of particular practical importance is the combination of small wavelength and low visocity as depicted in Fig. 2 d where the phase error is reduced by two orders of magnitude for the shortest wave as compared to the original cumulant method and the BGK methods.

7.2. Taylor-Green vortex

In our second test case, also adapted from [18], we investigate the decay of a planar Taylor-Green vortex in a constant flow field defined by:

$$u(t=0) = u_0 L_0/L + U L_0/L \sin(2\pi x/L)\cos(4\pi z/(3L)), \tag{131}$$

$$v(t=0) = 0, \tag{132}$$

$$w(t=0) = -3U/2L_0/L \cos(2\pi x/L)\sin(4\pi z/(3L)) \tag{133}$$

$$\rho(t=0) = \rho_0\left(1 + \frac{3U^2L_0^2}{2L^2\Delta x^2/\Delta t^2}(\cos(4\pi x/L) + \cos(8\pi z/(3L))\right). \tag{134}$$

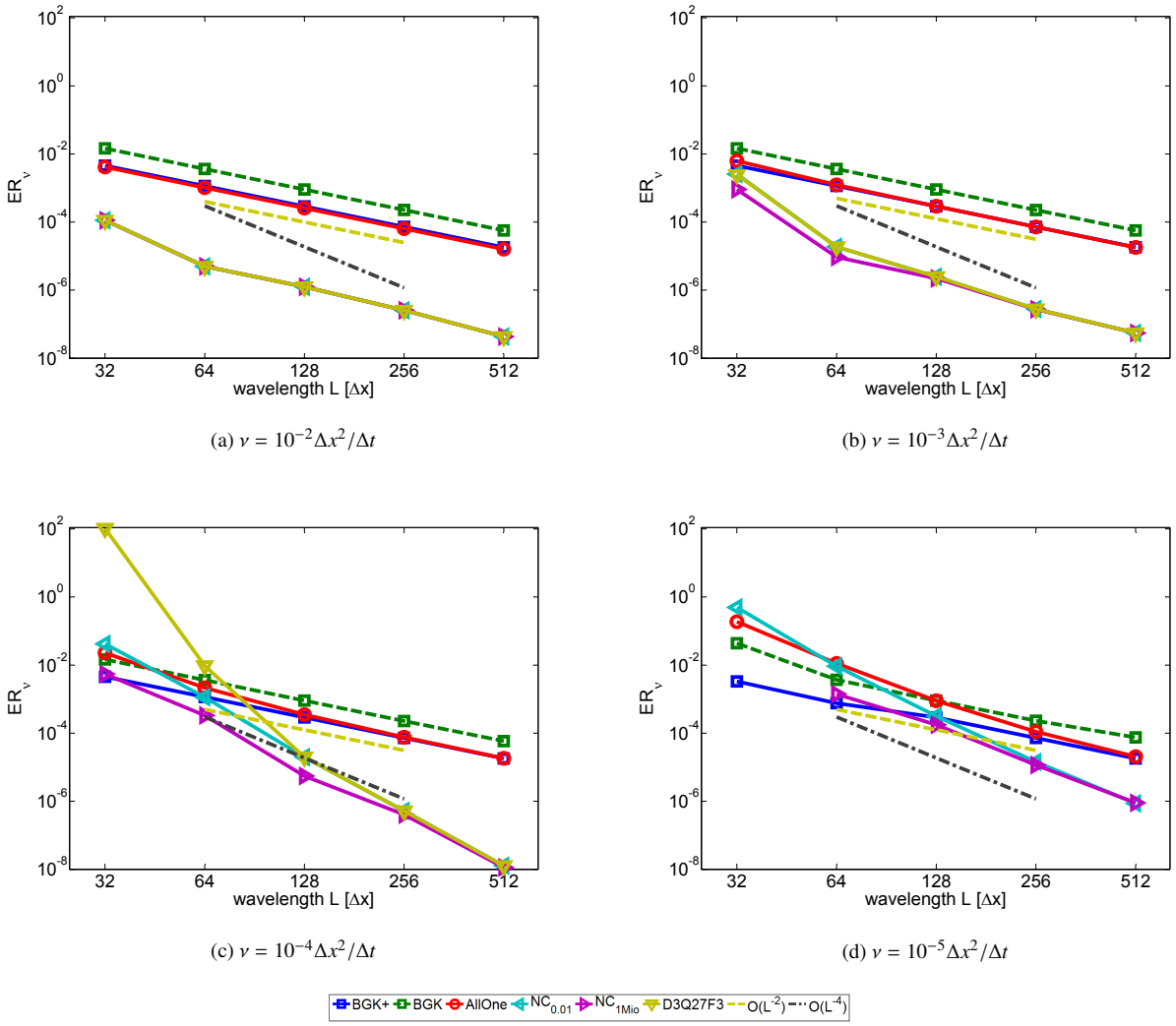

(a) $\nu = 10^{-2}\Delta x^2/\Delta t$

(b) $\nu = 10^{-3}\Delta x^2/\Delta t$

(c) $\nu = 10^{-4}\Delta x^2/\Delta t$

(d) $\nu = 10^{-5}\Delta x^2/\Delta t$

Figure 1: Convergence results of the error in viscosity using the double shear wave test case for various viscosities. From upper left to lower right: $\nu = \{10^{-2}, 10^{-3}, 10^{-4}, 10^{-5}\}\Delta x^2/\Delta t$. In the case of high viscosity, fourth order accuracy is not observed. This might be due to the fact the a term proportional to ν^3 was neglected in the linearized leading error. Still there is a significant improvement in the high viscosity regime with the magnitude of the error being more than two orders of magnitude lower than for all other tested methods. Note that the high viscosity case is close to the boundary of the stable interval $(1/42\Delta x^2/\Delta t)$. In the low viscosity regime fourth order accuracy is observed to at least a wavelength of $512\Delta x$. It is also observed that the BGK+ method with the equilibrium derived from cumulants is more accurate than the standard BGK method with Taylor-expanded equilibrium. The D3Q27F3 method with optimized parameters and adevection correction behaves identical to the method without advection correction until viscosity $\nu = 10^{-4}\Delta x^2/\Delta t$. For too low viscosities the method becomes unstable. No results for the D3Q27F3 method at $\nu = 10^{-5}\Delta x^2/\Delta t$ are plotted.

Again it is $L_0 = 32\Delta x$, $u_0 = 0.096\Delta x/\Delta t$ and $U = 0.001\Delta x/\Delta t$. The grid resolution is varied from $32\Delta x$ to $521\Delta x$ for four different viscosities. The decay of the amplitude is measured every $1000(L/L_0)^2$ time steps starting at time step $11000(L/L_0)^2$ and ending at time step $20000(L/L_0)^2$. The logarithm of the amplitude of the wave is fitted to a linear function from which the viscosity is recovered. The error in viscosity is reported in Fig. 3. In this test case both the BGK+ and the AllOne results show an apparent fourth order accuracy when the viscosity is small enough. This might be attributed to the leading error being a function of the viscosity such that it becomes irrelevant for small enough viscosity. Note that the standard BGK model is always only second order accurate. In the range where all models except of the standard BGK model have an apparent fourth order accuracy, the optimized parameters do not

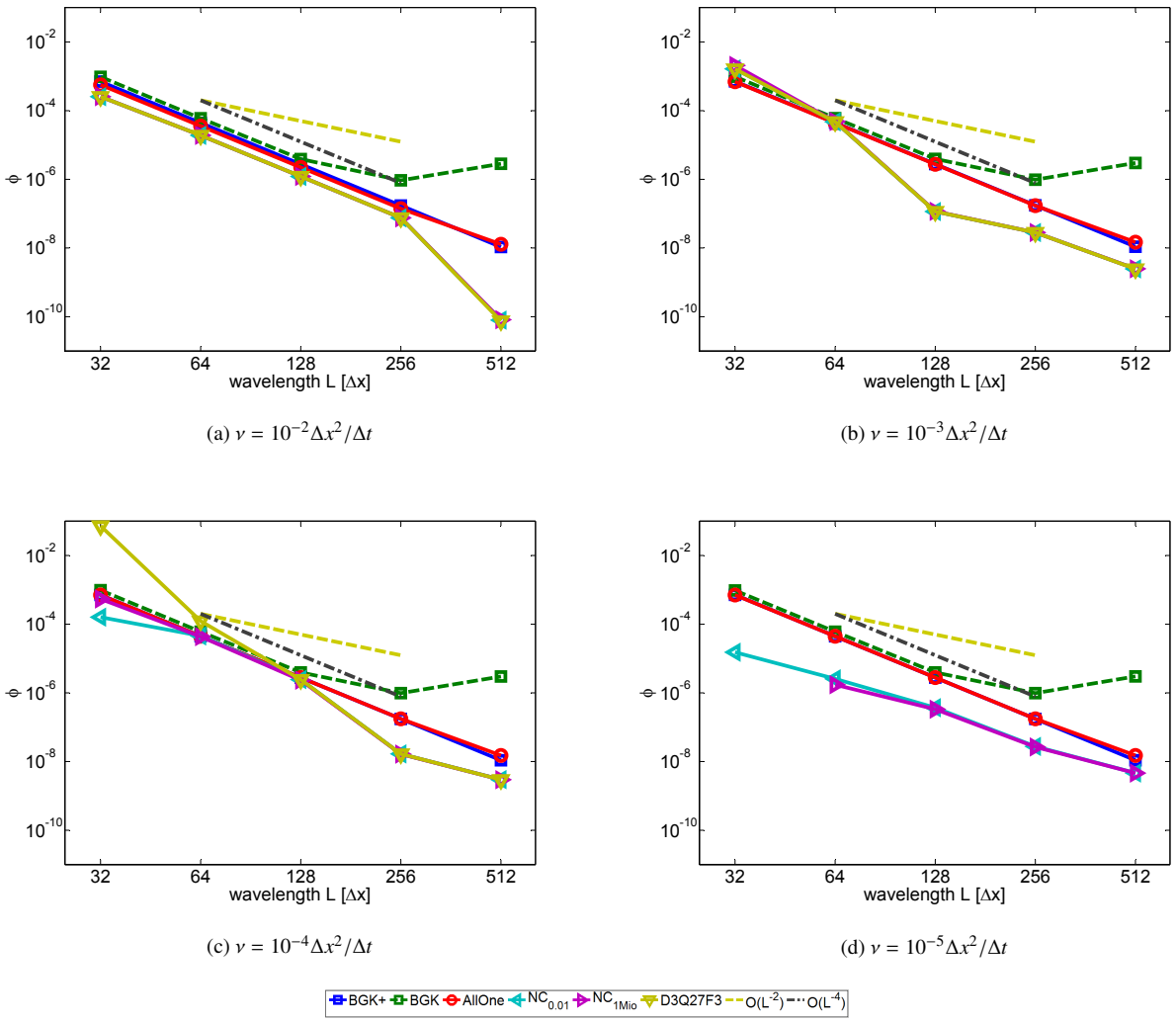

(a) $\nu = 10^{-2}\Delta x^2/\Delta t$

(b) $\nu = 10^{-3}\Delta x^2/\Delta t$

(c) $\nu = 10^{-4}\Delta x^2/\Delta t$

(d) $\nu = 10^{-5}\Delta x^2/\Delta t$

Figure 2: Convergence of the phase error of the double shear wave test case (same simulations as in Fig. 1). In general a fourth order accuracy is observed for most cases. In the case of the BGK method the phase error increases for very high resolutions. The parameters which were obtained in order to improve diffusion are either neural or positive for advection. In the high viscosity case with $\nu = 10^{-2}\Delta x^2/\Delta t$ the phase error of the optimized cumulant method is only half as large as the error of the non-optimized cumulant method. At the lowest viscosity the optimized parameters appear to improve the phase shift by two orders of magnitude for the shortest wavelength. Albeit the difference becomes smaller for longer wavelength. The advection correction has no positive influence in this test case as the error it is supposed to heal does not occur here.

seem to improve the results any further. However, in the range of larger viscosities the BGK+ and AllOne model show only second order accuracy while the optimized cumulant model obtains fourth order accuracy for short enough wavelength before the error saturates for wavelength larger than $128\Delta x$ for $\nu = 10^{-2}\Delta x^2/\Delta t$ and larger than $256\Delta x$ for $\nu = 10^{-3}\Delta x^2/\Delta t$. The existence of a post-asymptotic regime is expected, albeit we have no explanation why the error saturates at this particular resolution. The limiter does not seem to have any influence on the result in this case.

In the Taylor-Green test case we observe a marked difference between the optimized cumulant method without advection correction and with advection correction (D3Q27F3 model). The method with advection correction shows larger errors in the diffusion and the size of these errors increase for decreasing viscosity. However, the fourth order convergence is still obtained. In addition we observe that the advection correction deteriorates stability for the lower viscosities. No result was obtained for the coarsest resolution at $\nu = 10^{-5}\Delta x^2/\Delta t$ and the results for longer wavelength

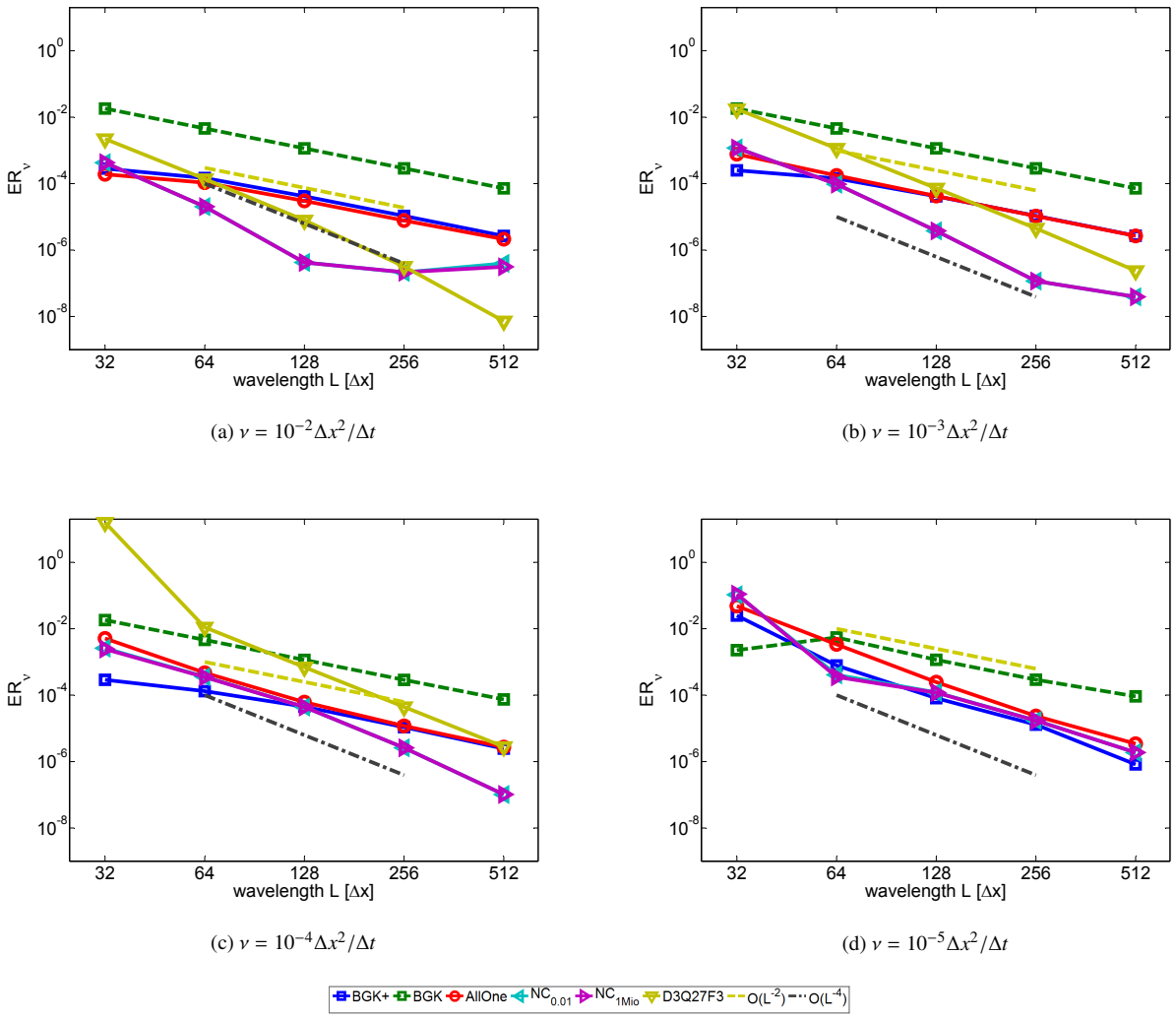

(a) $\nu = 10^{-2}\Delta x^2/\Delta t$

(b) $\nu = 10^{-3}\Delta x^2/\Delta t$

(c) $\nu = 10^{-4}\Delta x^2/\Delta t$

(d) $\nu = 10^{-5}\Delta x^2/\Delta t$

Figure 3: Convergence results of the error in viscosity using the Taylor-Green test case for various viscosities. From upper left to lower right: $\nu = \{10^{-2}, 10^{-3}, 10^{-4}, 10^{-5}\}\Delta x^2/\Delta t$. For low enough viscosity all models based on cumulants (this includes BGK+) are apparently of fourth order. The standard BGK method remains second order accurate at all viscosities. Only the optimized cumulant method appears to be fourth order accurate for all viscosities, albeit it is observed that the error saturates for the higher viscosities at longer wavelength. The value of the limiter does not seem to affect the accuracy of the method in this example. The error of the cumulant method with advection correction increases with decreasing viscosity, but this does not seem to interfere with the convergence order. The irregular error at $L = 30\Delta x$ and viscosity $\nu = 10^{-4}\Delta x^2/\Delta t$ could be identified as the onset of instability by inspection of the velocity field. No data for the D3Q27F method are shown for $\nu = 10^{-5}\Delta x^2/\Delta t$ as the method was not stable for that viscosity.

have been disregarded here as they deviated too strongly from the analytical solution. However, looking at Fig. 4 we see the advantage of the advection correction. The phase shift is considerable reduced by the advection correction. At the same time no convergence is seen as the error saturates very quickly at a value of 10^{-6} radian for traveling three times its own diameter. An orthodox interpretation of asymptotics judges a method with an error independent of resolution as inconsistent. However, in our case we see that the error in the D3Q27F3, albeit constant for long waves, is several orders of magnitudes smaller than in the uncorrected case. In fact, even at the highest resolution with a wavelength of $512\Delta x$ the phase error in the advection corrected method is still two orders of magnitude smaller than in the uncorrected methods.

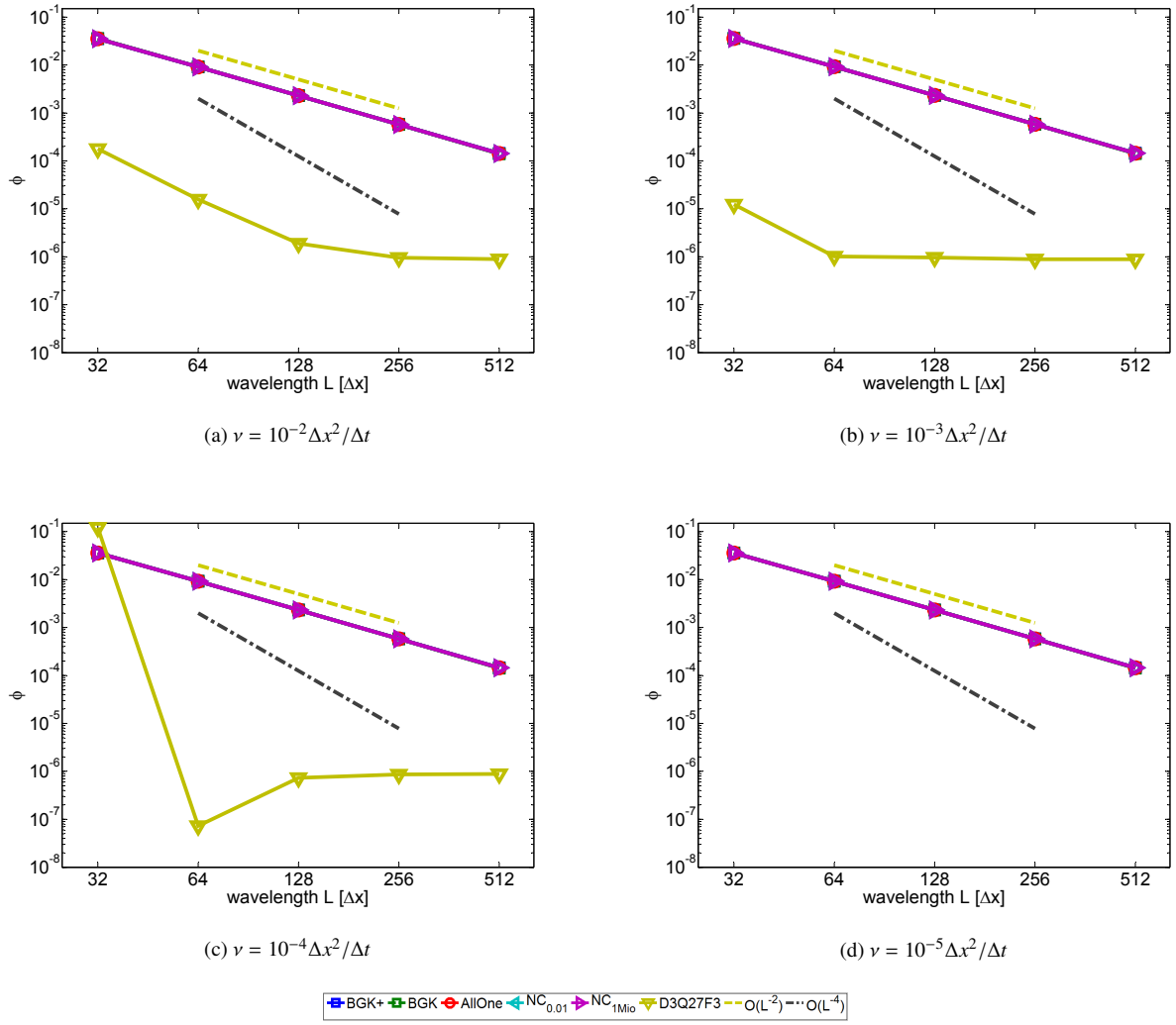

(a) $\nu = 10^{-2}\Delta x^2/\Delta t$

(b) $\nu = 10^{-3}\Delta x^2/\Delta t$

(c) $\nu = 10^{-4}\Delta x^2/\Delta t$

(d) $\nu = 10^{-5}\Delta x^2/\Delta t$

Figure 4: Convergence results of the phase shift after the vortex traveled three times its own diameterin the Taylor-Green test case (same simulations as in Fig. 3). This test highlights the remaining leading order error in advection due to the finite isotropy of the D3Q27 lattice. Unlike in the double shear wave test, the phase converges only with the second order of accuracy. It is observed that the optimal parametrization has no influence on the phase error. The phase error can be eliminated to leading order by the advection correction used in the D3Q27F3 model. This model is hence expected to be fourth order accurate in diffusion and in advection. However, the fourth order accuracy in advection is not seen here as the phase error of the corrected scheme saturates very quickly at 10^{-6} radians for each time the vortex travels three times its own diameter. Compared to the uncorrected schemes this residual error is extremely small.

It should be noted that by using the *traveling* shear wave and the *traveling* Taylor-Green vortex which are advected by a constant velocity we probe the Galilean invariance of our model also in a different way. As has been discussed in detail in [18] the cumulant method and the BGK+ method do not suffer from the cubic dependency of the viscosity from the Mach number which is a known defect of the standard BGK and MRT methods. This is also confirmed by the current results since the defect would be of second order in diffusive scaling. This means fourth order convergence would be impossible for the two test cases shown here if the cumulant method had inherited the viscosity defect from the BGK method. Our result also confirms that this property is retained for the cumulant method with optimal parametrization. This is essentially a consequence of the fact that cumulants are Galilean invariant independent of the relationships between the relaxation rates. Note that this is not the case for the usual MRT method as discussed

in detail in [18]. The consequence of the spurious dependence of the viscosity on the Mach number is seen in Fig. 3 plot (d). Here the BGK+ method is apparently fourth order accurate while the BGK method is still second order accurate. The only difference between the two methods is that the cubic in Mach number viscosity defect has been removed from the BGK+ method. So the difference in their respective convergence must come from their difference in Galilean invariance.

As a last example we check how the error in viscosity behaves when we change the Mach number under fixed Reynolds number and fixed resolution. For this we repeat the computation of the Taylor-Green vortex now in Mach number scaling:

$$
\begin{aligned}
u(t=0) &= u_0 U/U_0 + U^2/U_0 \sin(2\pi x/L)\cos(4\pi z/(3L)), && (135)\\
v(t=0) &= 0, && (136)\\
w(t=0) &= -3U^2/(2U_0)\cos(2\pi x/L)\sin(4\pi z/(3L)) && (137)\\
\rho(t=0) &= \rho_0\left(1+\frac{3U^4}{2U_0^2\Delta x^2/\Delta t^2}(\cos(4\pi x/L)+\cos(8\pi z/(3L))\right). && (138)
\end{aligned}
$$

We use $U_0 = 0.001\Delta x/\Delta t$ and run the simulations for $200000U_0/U\Delta t$. The measurements starts at $11000U_0/U\Delta t$. The Reynolds number studied is $Re = L_0U_0/(10^{-4}\Delta x^2/\Delta t) = 320$. The cases $L = L_0$ and $L = 2L_0$ are considerd. The results are shown in Fig. 5. At this relatively high Reynolds number for such coarse grids, the optimized cumulant method is seen to have a larger error for a large Mach number than the BGK+ method. However, at lower Mach number the error in the optimized cumulant method reduces to a significantly lower value while the error of the BGK+ method remains stable up to the point where the method becomes unstable due to too low viscosity. The AllOne method shows increasing errors for lower Mach numbers. The explanation for this is that the relationship between the relaxation rates becomes increasingly unfavorable when ω_1 is reduced while all the other rates are kept constant. As a result, the AllOne method does not seem to benefit from small time steps or low Mach numbers in the same way as the optimized method does. This behavior was first observed by Dellar [55] in the context of the MRT lattice Boltzmann method. The situation for the BGK+ method is actually even less favorable. What is not seen directly in the figure is that the BGK/BGK+ method suffers from pressure oscillations that grow with decreasing Mach number at fixed resolution and Reynolds number, which eventually leads to a catastrophic failure of the method when the Mach number is too low. It is often falsely claimed in literature that the lattice Boltzmann method should be run with as small a Mach number as possible to increase the accuracy. In reality, the convergence of the lattice Boltzmann method is subject to certain conditions, i.e. diffusive scaling. Under pure Mach number scaling no convergence is predicted by the theory such that those results do not disqualify the methods in general. Still it is undesirable for a numerical method to deteriorate for smaller time steps and despite the fact that this behavior is well known for a long time it sees little discussion in literature, perhaps due to the fact that it would put the lattice Boltzmann method in a bad light. As already mentioned by Dellar [55] more than a decade ago, the problem can be solved by scaling the relaxation rates of the ghost modes together with the Mach number. This is of course automatically done when using the optimized parameters and hence the optimized cumulant method shows the desired behavior of decreasing errors with decreasing Mach number. It can be conjectured from the results in Fig. 5 that the convergence studies shown in the previous plots would be more in favor of our new method if we started our convergence study from a lower initial Mach number. However, this would have increased the computational cost beyond an acceptable level.

In general we observe a substantial reduction of the error through the optimized parameters compared to AllOne and BGK+ unless for those cases where AllOne and BGK+ have apparent fourth order accuracy. It is also observed that in all cases where the error is very small, the error deviates from a straight line, indicating that we arrived at a level of accuracy where the residual error is influenced by numerical effects such as round-off errors.

8. Conclusions

Only mutually statistically independent observable quantities can evolve on mutually independent time scales. Cumulants are by design mutually independent observable quantities. They are used as the starting point for a new multi-relaxation time lattice Boltzmann model. The new free relaxation rates are adjusted to eliminate the linearized

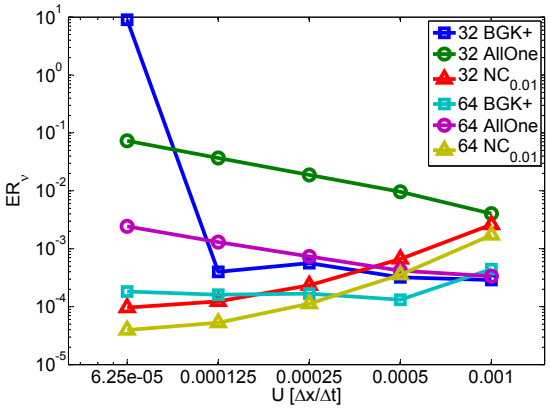

Figure 5: The viscosity error for different Mach numbers at fixed Reynolds number and fixed resolution, with $L = 32\Delta x$ and $L = 64\Delta x$. The amplitude of the vortex velocity is U and the superimposed advection velocity is $96U$. We show only data for BGK+, AllOne and the optimized cumulant method $\mathrm{NC}_{0.01}$. It is observed that the optimized cumulant method benefits the most from low Mach numbers. The AllOne method shows increasing errors with decreasing Mach number at fixed Reynolds number due to an increasingly unfavorable relation between the changing relaxation rate ω_1 and the fixed rates for other cumulants. The BGK+ method becomes unstable for too low Mach numbers.

leading error in the diffusion. The exact error term is derived by Taylor expansion and it is seen that it can be reduced to five independent terms that can be set simultaneously to zero by a specific choice of five independent parameters. Since the error depends only on the value of three independent relaxation rates it was necessary to introduce two artificial parameters in the equilibrium of the fourth order cumulants. Despite the fact that magic or quartic parameters have been researched for more than 20 years, our solution is the first general solution that eliminates a certain class of errors completely under the condition of small enough viscosity.

The condition of small viscosity arises from the neglect of terms $\propto \nu^3$ in the linearized leading error. The computer algebra system was also able to determine a solution without neglecting these terms but the result was too complicated to be considered for implementation. Since we are primarily interested in the simulation of turbulent flow where the viscosity is very small, a residual leading error proportional to the third power in viscosity is irrelevant for us. In fact, for viscosities of $10^{-4}\Delta x^2/\Delta t$ and smaller the residual error was not measurable with a shear wave or a vortex even for long wavelength.

The solution presented here determines all relaxation rates of third order cumulants. For very low viscosities all these rates approach zero. The optimized case is less stable than the case with all rates set to one. Stability can be restored through a limiter as described above. The limiter requires a threshold value for each cumulant such that the number of undetermined parameters of the method did not reduce. Instead of having three undetermined relaxation rates we need to choose three thresholds. This is still an advantage considering the fact that fourth order accuracy is obtained only for one specific set of relaxation rates while it is obtained for all positive values of the thresholds. In that way we reduced the sensitivity of the error on the free parameters considerably. It is confirmed by our experiments that the limiter affects the accuracy only weakly.

The essential advantage of a quartic parametrization over other methods to enhance the convergence order (e.g. by enlarging the velocity set or by adding correction terms through additional finite differences) is that the quartic parametrization has zero computational overhead. The necessary relaxation parameters can be computed once at the start of the simulation. We observe only a small overhead of 1.5% in the update rate, most likely due to the application of the limiter. Note that we did not focus on code optimization and that optimized lattice Boltzmann method are usually memory bound algorithms [56, 57, 58, 59, 60].

The ability to obtain fourth order accuracy for diffusion with a stencil that accesses only the 26 nearest neighbors distinguishes the lattice Boltzmann method from finite difference methods. In that way, the presented method can also be viewed as an answer to the question what we gain by utilizing the velocity distribution function instead of the macroscopic quantities when solving the Navier-Stokes equation [61, 62]. The lattice Boltzmann method can exploit the information on higher derivatives of the velocity contained in the distribution function in order to enhance the

accuracy to a level beyond that obtained by finite differences [63]. In comparison, a finite difference method would require a larger stencil accessing more neighbors to obtain fourth order accuracy.

Our method to obtain fourth order accuracy in diffusion is readily combined with a method to ensure fourth order accuracy in advection [53]. In the current paper we show only preliminary results by compensating the errors in advection through finite differences. It is observed that removing the errors in advection in this way reduces the accuracy with regard to diffusion without affecting the convergence order. The model is found to be fourth order accurate in diffusion while it has a very small error in advection for which no clear convergence order is seen experimentally. The relation between the residual errors in the two domains might not be optimal yet and future research will focus on the search of a better compromise. We note that, even though the deterioration of the diffusion due to the improved advection is significant when compared to the fourth order accurate method without advection correction, at moderate viscosities, the errors in diffusion are still smaller than in the standard BGK method.

It is an interesting fact that the solution we present here in three dimensions has no matching solution for the two dimensional case. In fact, it appears to be impossible to obtain fourth order accurate diffusion in two dimensions without enlarging the neighborhood of the lattice node. The non-existence of a solution in 2D might came as a surprise to some but we have to remind that fourth order cumulants behave differently in two and three dimensions. For that reason, there is no difference between the central moment method and the cumulant method in two dimensions whereas there is a drastic difference between both methods in three dimensions. The non-existence of a solution in two dimensions should remind us that it is not always possible to generalize from two to three dimensions and not even vice versa.

The theory presented here is readily applied to actual turbulent simulations as we show in the second part of the series by simulating the flow around a sphere at drag crisis [24].

Acknowledgments

We thank Hussein Ali Hussein, Stephan Lenz and Jon McCullough for proofreading the manuscript and Martin Gehrke for pointing out some misprints in the equations. The research was funded by the TU Braunschweig.

Appendix A. Transformation between raw moments and linearized cumulants

The cumulant transform is non-linear and so are the transformations from moments to cumulants and back. Since we are concerned with the linear diffusion part of the Navier-Stokes equation it is admissible to linearize the transformations around equilibrium (i.e. zero for all non-conserved cumulants). In order to do this we first list the raw moments expressed in terms of cumulants and omit equations that can be obtained by permuting the indexes:

$$m_{000} = \rho, \tag{A.1}$$
$$m_{100} = \rho u, \tag{A.2}$$
$$m_{110} = \rho(uv + c_{110}), \tag{A.3}$$
$$m_{200} = \rho(u^2 + c_{200}), \tag{A.4}$$
$$m_{210} = \rho(u^2 v + 2uc_{110} + vc_{200} + c_{210}), \tag{A.5}$$
$$m_{111} = \rho(uvw + uc_{011} + vc_{101} + wc_{110} + c_{111}), \tag{A.6}$$
$$m_{220} = \rho(u^2 v^2 + u^2 c_{020} + 4uvc_{110} + 2c_{110}^2 + 2uc_{120} + v^2 c_{200} + c_{020}c_{200} + 2vc_{210} + c_{220}), \tag{A.7}$$
$$m_{211} = \rho(u^2(vw + c_{011}) + 2c_{101}c_{110} + 2u(vc_{101} + wc_{110} + c_{111}) + vwc_{200} + c_{011}c_{200} + vc_{210} + wc_{201} + c_{211}). \tag{A.8}$$

A linearization around equilibrium thereof and keeping velocity terms until second order in u, v and w gives:

$$\hat{m}_{000} = \rho, \tag{A.9}$$
$$\hat{m}_{100} = \rho u, \tag{A.10}$$
$$\hat{m}_{110} = \rho(uv + c_{110}), \tag{A.11}$$
$$\hat{m}_{200} = \rho(u^2 + c_{200}), \tag{A.12}$$
$$\hat{m}_{210} = \rho(v/3 + c_{210}), \tag{A.13}$$
$$\hat{m}_{111} = \rho c_{111}, \tag{A.14}$$
$$\hat{m}_{220} = \rho(u^2/3 + v^2/3 + (c_{200} + c_{020})/3 - 1/9 + c_{220}), \tag{A.15}$$
$$\hat{m}_{211} = \rho(vw/3 + c_{011}/3 + c_{211}). \tag{A.16}$$

We restrict ourselves to moments up to order four since higher orders do not appear in our expansion.

Next we list all non conserved cumulants in terms of raw moments and the conserved quantities up to order four. Cumulants that can be obtained by permuting the indexes from those listed are omitted:

$$c_{200} = m_{200}\rho^{-1} - u^2, \tag{A.17}$$
$$c_{110} = m_{110}\rho^{-1} - uv, \tag{A.18}$$
$$c_{111} = \rho^{-1}(m_{111} - um_{011} - vm_{101} - wm_{110}) + 2uvw, \tag{A.19}$$
$$c_{120} = \rho^{-1}(m_{120} - 2um_{110} - vm_{200} - wm_{110}) + 2u^2w, \tag{A.20}$$
$$c_{220} = \rho^{-1}(m_{220} + 2u^2m_{020} + v^2m_{200} - 2(um_{120} + vm_{210} + m_{110}^2\rho^{-1}) + 8uv - m_{020}m_{200}) - 6u^2v^2, \tag{A.21}$$
$$c_{211} = \rho^{-1}(m_{211} - vm_{201} - wm_{210} - m_{011}m_{200}\rho^{-1} - 2(um_{111} - vwm_{200} + m_{101}m_{110}\rho^{-1} - u^2m_{011}) + 4u(vm_{101} + wm_{110})) - 6u^2vw. \tag{A.22}$$

From this we can deduce the linearized collision operator of the cumulants $\hat{\Omega}^{\mathrm{c}}_{\alpha\beta\gamma}$ in terms of the collision operator of the moments $\Omega^{\mathrm{m}}_{\alpha\beta\gamma}$:

$$\hat{\Omega}^{\mathrm{c}}_{200} = \Omega^{\mathrm{m}}_{200}, \tag{A.23}$$
$$\hat{\Omega}^{\mathrm{c}}_{110} = \Omega^{\mathrm{m}}_{110}, \tag{A.24}$$
$$\hat{\Omega}^{\mathrm{c}}_{111} = \Omega^{\mathrm{m}}_{111}, \tag{A.25}$$
$$\hat{\Omega}^{\mathrm{c}}_{210} = \Omega^{\mathrm{m}}_{210}, \tag{A.26}$$
$$\hat{\Omega}^{\mathrm{c}}_{220} = \Omega^{\mathrm{m}}_{220} - (\Omega^{\mathrm{m}}_{200} + \Omega^{\mathrm{m}}_{020})/3, \tag{A.27}$$
$$\hat{\Omega}^{\mathrm{c}}_{211} = \Omega^{\mathrm{m}}_{211} - \Omega^{\mathrm{m}}_{011}/3. \tag{A.28}$$

Choosing the moment m_{211} as an example we use (A.16) to deduce:

$$\bar{m}_{211} = \rho(vw/3 + \bar{c}_{011}/3 + c_{\bar{2}11}) = \rho vw/3 + \bar{C}_{011}/3 + \bar{C}_{211}. \tag{A.29}$$

Using (80) we write:

$$\bar{m}_{211} = \rho vw/3 + C^{eq}_{011}/3 - \tau_1\Omega^{\mathrm{c}}_{011}/3 + C^{eq}_{211} - \tau_8\Omega^{\mathrm{c}}_{211}. \tag{A.30}$$

It is obvious that $C^{eq}_{011} = 0$. The fourth order cumulant is not zero due to the introduced modification: $C^{eq}_{211} = B\bar{C}_{011}$. Hence:

$$\bar{m}_{211} = \rho vw/3 - \tau_1\Omega^{\mathrm{c}}_{011}/3 - B\tau_1\Omega^{\mathrm{c}}_{011} - \tau_8\Omega^{\mathrm{c}}_{211}. \tag{A.31}$$

Using (A.28) and the permutation of (A.24) yields:

$$\bar{m}_{211} = \rho vw/3 - \tau_1\Omega^{\mathrm{m}}_{011}/3 - B\tau_1\Omega^{\mathrm{m}}_{011} - \tau_8(\Omega^{\mathrm{m}}_{211} - \Omega^{\mathrm{m}}_{011}/3), \tag{A.32}$$

which is how (91) was obtained.

Appendix B. Leading errors in advection

The order of the error in advection is dictated by the lowest order cumulants that cannot be chosen independently. An asymptotic analysis similar to the one presented in section 5.2 shows us that for obtaining fourth order accuracy in advection, all third order cumulants have to vanish in equilibrium until $O(Ma^3)$ and all fourth order cumulants have to vanish until $O(Ma^2)$. However, due to the finite number of speeds in the D3Q27 lattice several third and fourth order cumulants cannot be set independently. As we discuss in [18] and elaborate on in [53], this has two consequences for the Galilean invariance: first there is a defect causing the viscosity to depend on the flow velocity. This problem is well understood and it has been solved [18, 64] by introducing a correction term into the equilibrium of the second order cumulants, i.e. equations (34)-(36). This error is hence no longer present in the method discussed in the paper. This is also evident from Fig. 1 and Fig. 3 which show the errors in viscosity of a traveling shear wave and a traveling vortex, respectively under diffusive scaling. Any error of $O(Ma^2)$ would obviously spoil the fourth order accuracy.

The second problem introduced due to the lack of the complete fourth order Galilean invariance is a phase lag in the traveling vortex test case. This defect was discussed qualitatively (without including all relevant terms) in [18]. The phase lag can be eliminated in the same way the defect in the viscosity was eliminated, by introducing a correction to the second order cumulants. This changes equations (34)-(36) in the collision operator to:

$$\begin{aligned}
C^*_{200} - C^*_{020} &= (1-\omega_1)(C_{200} - C_{020}) - 3\rho\left(1-\frac{\omega_1}{2}\right)(u^2 D_x u - v^2 D_y v) \\
&\quad +\rho\omega_1\left(2\left(\frac{1}{\omega_1}-\frac{1}{2}\right)^2 - \frac{1}{6}\right)((D_x u)^2 + u D_{xx} u - (D_y v)^2 - v D_{yy} v), \qquad \text{(B.1)} \\
C^*_{200} - C^*_{002} &= (1-\omega_1)(C_{200} - C_{002}) - 3\rho\left(1-\frac{\omega_1}{2}\right)(u^2 D_x u - w^2 D_z w) \\
&\quad +\rho\omega_1\left(2\left(\frac{1}{\omega_1}-\frac{1}{2}\right)^2 - \frac{1}{6}\right)((D_x u)^2 + u D_{xx} u - (D_z w)^2 - w D_{zz} w), \qquad \text{(B.2)} \\
C^*_{200} + C^*_{020} + C^*_{002} &= \kappa_{000}\omega_2 + (1-\omega_2)(C_{200} + C_{020} + C_{002}) - 3\rho\left(1-\frac{\omega_2}{2}\right)(u^2 D_x u + v^2 D_y v + w^2 D_z w) \\
&\quad +\rho\frac{6 - 3(\omega_1+\omega_2) + \omega_1\omega_2}{3\omega_1}((D_x u)^2 + u D_{xx} u + (D_y v)^2 + v D_{yy} v + (D_z w)^2 + w D_{zz} w). \qquad \text{(B.3)}
\end{aligned}$$

The only difficulty in computing (B.1) - (B.3) is to determine the second derivatives of velocity $D_{xx}u$ and so on, which can, of course, be done by finite differences. It is of note that the corrections involving second derivatives in velocity are not small even if the viscosity is small, i.e. for $\omega_1 \to 2$. The first derivatives of velocity appearing in (B.1) - (B.3), can be computed directly from the non-equilibrium distributions via (27) - (29) by the same principle which is applied in certain turbulence models [65, 66, 67] and in certain phase field models for the computation of the gradient of the phase indicator [68, 69, 70].

Appendix C. Linearized Leading Error in two dimensions

Let us regard the two dimensional projection of the D3Q27 lattice which is the D2Q9 lattice. This model has only two independent cumulants of order three (C_{12} and C_{21}) and only one fourth order cumulant (C_{22}). The fourth order cumulant is isotropic which means that its equilibrium can only depend on the isotropic part of the stress $\partial_x u + \partial_y v$. However, the isotropic part of the stress is zero to second order such that C_{22} offers no degree of freedom for the optimization. Due to symmetry constraints the relaxation rates for C_{12} and C_{21} have to be identical such that the optimization problem has only a single degree of freedom in two dimensions whereas it has five degrees of freedom in three dimensions. At the same time some of the derivatives vanish in two dimensions from the *LLE*. To see this we rewrite the LLE_x for the two dimensional projection by setting $\tau_4 \to \tau_3$ and by eliminating all derivatives in z direction in (101):

$$
\begin{aligned}
LLE_{x2D} &= \left[\frac{\tau_1}{36} - \frac{2\tau_3\tau_1^2}{9} + \frac{\tau_1^3}{9}\right]\partial_{yyyy}u + \\
&\frac{1}{54}[\tau_2 + 2\tau_1 - 12\tau_1\tau_3(\tau_1+\tau_2) + 12\tau_1^3]\partial_{xxyy}u + \\
&\frac{1}{108}[2\tau_2(12\tau_1\tau_3 - 1) + 24\tau_1^2\tau_3 + 12\tau_1^3]\partial_{xxxx}u. \qquad \text{(C.1)}
\end{aligned}
$$

The corresponding system of equations, ignoring τ_1^3, is:

$$
\begin{aligned}
0 &= \frac{\tau_1}{36} - \frac{2\tau_3\tau_1^2}{9}, \qquad \text{(C.2)}\\
0 &= \tau_2 + 2\tau_1 - 12\tau_1\tau_3(\tau_1+\tau_2), \qquad \text{(C.3)}\\
0 &= 2\tau_2(12\tau_1\tau_3 - 1) + 24\tau_1^2\tau_3, \qquad \text{(C.4)}
\end{aligned}
$$

which is easily seen to possess no solution in τ_3. We hence conclude that while there exists a solution that permits fourth order accurate diffusion in three dimension no such solution exists in two dimensions. It is, of course, possible to solve two dimensional problems with the three dimensional method and periodic boundary conditions in the third dimension. Another possibility is to look for a special case such like a shear wave for which it is known that certain derivatives disappear such that we can solve the equations of the *LLE* independently. For example, if we restrict ourselves to the TRT ansatz in which $\tau_1 = \tau_2$ and solve (C.2)-(C.4) individually we obtain for (C.2):

$$\tau_3 = \frac{1}{8\tau_1}, \qquad \text{(C.5)}$$

for (C.3):

$$\tau_3 = \frac{1}{8\tau_1}, \qquad \text{(C.6)}$$

and for (C.4):

$$\tau_3 = \frac{3}{16\tau_1}. \qquad \text{(C.7)}$$

It is promising that the roots for (C.2) and (C.3) are the same, but both are incompatible with the root of (C.4) and this renders the result useless for the general case. It is, however, interesting that these results can be expressed in terms of (69) as constants. The errors in $\partial_{yyyy}u$ and $\partial_{xxyy}u$ vanish for:

$$\Lambda_{oe} = \tau_1\tau_3 = \frac{1}{8}. \qquad \text{(C.8)}$$

The error in $\partial_{xxxx}u$ vanishes for:

$$\Lambda_{oe} = \tau_1\tau_3 = \frac{3}{16}. \qquad \text{(C.9)}$$

In contrast, our general solution (112) -(116) cannot be expressed through constant parameters Λ_{oe}.

As a final remark in the context of the D2Q9 lattice we point the reader to a formally fourth order accurate solution to the diffusion problem on this lattice by Dubois et al. [71]. To obtain this solution the speed of sound had to be redefined and the viscosity had to be tuned to a constant and impractically high value. We do not see this solution in our case since we do not consider the speed of sound as a free parameter as this would have severe implications on Galilean invariance. It is interesting that a formal solution to the problem exists but it is not a feasible solution for actual computations.

Appendix D. Linearized Leading Error from steady state assumption

Results obtained for the advection diffusion equation [45, 13] imply that an optimization with regard to steady state was sufficient if the transport coefficients were small enough. To check whether this is true for our case we eliminated the expansion with regard to time in (77) and derived the corresponding LLE^{steady}:

$$\begin{aligned}
LLE_x^{steady} &= \left[\frac{\tau_1}{18} - \frac{(\tau_3+\tau_4)\tau_1^2}{9} - \frac{(\tau_4+\tau_3)B\tau_1^2}{6}\right](\partial_{zzzz}u + \partial_{yyyy}u) \\
&+ \left[\frac{\tau_1}{9} + \frac{B\tau_1}{6} - \frac{2(\tau_3-\tau_4)\tau_1^2}{9} - \frac{B(\tau_3+\tau_4)\tau_1^2}{3} - \frac{(4+12B)\tau_5\tau_2^2}{9}\right]\partial_{yyzz}u \\
&+ \frac{1}{108}[\tau_2(2+24(A-1-B)\tau_1\tau_3) + \tau_1(27B-2-18A \\
&+ 12\tau_1(4(A-1-B)\tau_3 + (10+12A-9B)\tau_4 - 4(1+3B)\tau_5))](\partial_{xyzz}v + \partial_{xyyz}w) \\
&+ \frac{1}{54}[\tau_2(1+12(A-1-B)\tau_1\tau_3) + \tau_1(5+3\tau_1((2A+B)\tau_3 + (3B-4-6A)\tau_4))](\partial_{xxyy}u + \partial_{xxzz}u) \\
&+ \frac{1}{108}[\tau_2(24(1-A+B)\tau_1\tau_3 - 2) + 4\tau_1(-1+3\tau_1((2A+B)\tau_3 + (2-3B)\tau_4))]\partial_{xxxx}u. \qquad \text{(D.1)}
\end{aligned}$$

It is observed that the terms $\propto \tau_1^3$ disappear when the analysis starts from the steady state. However, this is not found to be the only difference. To check whether (D.2) is a good approximation of (101) for small τ_1 we obtain the set of equations equivalent to (106) and solve for τ_3, τ_4, τ_5, A and B. The results are not shown here as they turn out to be significantly more complicated then the solution we obtained from (101). Nevertheless we substitute all parameters obtained from (D.2) into (101) in order to see whether the resulting *LLE* is small. We obtain:

$$LLE_x^{steady\to trans} = \frac{4\tau_1^3 - \tau_1}{36}(\partial_{yyyy}u + \partial_{zzzz}u + \partial_{xxxx}u + 2(\partial_{yyzz}u + \partial_{xxyy}u + \partial_{xxzz}u)). \qquad \text{(D.2)}$$

While this becomes indeed smaller with smaller viscosity, it does so only linearly which is insufficient. It merely means that the hyper-viscosity is proportional to the viscosity and this does not imply fourth order accuracy in the limit of small viscosities. Instead, our result confirms the importance of the consideration of the transient nature of the lattice Boltzmann equation in the analysis.

Appendix E. Update rate

Here we present some update rate figures for our method. All test cases were implemented in a code with indirect addressing using the EsoTwist data structure [72] in CUDA. The code [73] was run on a Nvidia Tesla K40c GPU in single and double precision and on a GeForce Titan X (Maxwell GM200) in single precision. We show only data obtained with the Taylor-Green vortex at the resolution $3\times512\times512$ lattice nodes. Note that this test case is too small to exploit the hardware performance. We are only interested in the difference between the update rates of the different models. The update rate is measured in Million Node Updates Per Second (MNUPS). The results are listed in Tab. E.1. The computational overhead of the revised cumulant method over the original cumulant method amounts to a difference of 1.5% in terms of update rate for computations in double precision. We assume that this difference comes mainly from the application of the limiter for the relaxation rates of the third order cumulants. For the comparison in double precision the BGK method has a 2.8 times higher update rate than the cumulant method. This gap shrinks to 2.6 times the update rate of the BGK in single precision. The overhead of the computation of the finite differences in the D3Q27F3 method reduces the update rate only by 10% for double precision, which is encouraging for indirect addressing. However, this difference increases to 28% when single precision is used. The Titan X card has more hardware registers than the K40c which is favorable for codes with more complex calculations. As a result we see that the BGK method is only 1.7 times as fast as the cumulant method. At the same time we observe some surprising behavior of the Titan X. For example, we find that running exactly the same code with a different value for the limiter

changes the update rate by as much as three percent. This is not observed in the K40c simulations. It is to be noted that the K40c card is a device intended for scientific computation whereas the Titan X card is a consumer graphics card. The Titan X card has no proper double precision support and dynamically alters the clock rate to give maximum performance without much concern for reproducibility. These numbers should hence not be taken too seriously. We show them anyway to highlight the fact that the ratio of the update rates between two different lattice Boltzmann kernels is a strong function of the hardware on which the comparison is made.

Even though the update rate is often equated with performance in literature, we stress here that only two methods with equal accuracy can be compared directly in such terms. In fact, accuracy is a much better performance indicator than update rate as a higher accuracy allows us to obtain a better result on a coarser grid. In particular, the so called curse of dimensionality acts in favor for methods of higher accuracy. In three spatial dimensions and using the optimistic acoustic scaling with $\Delta t \propto \Delta x$ the required number of node updates to solve a given physical problem scales like Δx^{-4}. This means, in order for the cumulant method to run as fast as the BGK method (under the most pessimistic ratio of update rates measured here) we have to increase the grid spacing to $2.8^{1/4}\Delta x_{BGK} \sim 1.29\Delta x_{BGK}$. The break even point in run time is hence reached by increasing the grid spacing by just 30%. At the same time we observe that the errors in the cumulant method are drastically lower than in the BGK method even at drastically lower resolutions. As a specific example we consider the results for the Taylor-Green vortex at a viscosity $\nu = 10^{-3}\Delta x^2/\Delta t$ as depicted in Fig. 3 (b). The BGK method requires 256 lattice nodes in one dimension to reach the same accuracy as the optimized cumulant method has for 32 lattice nodes. Due to the curse of dimensionality the BGK method requires 4096 more node updates than the optimized cumulant method to obtain the same result with the same accuracy. Even if the BGK update rate is three times larger than the one of the cumulant method, the BGK method is still more than thousand times slower.

hardware	precision	BGK	BGK+	AllOne	$NC_{0.01}$	NC_{1Mio}	D3Q27F3
K40c	double	451.2	438.8	161.5	159.1	159.1	149.9
K40c	single	762.2	661.4	294.4	279.2	279.2	202.1
Titan X	single	1303.5	1326.2	822.6	775.4	753.3	602.9

Table E.1: Update rates in Million Node Updates Per Second of the different LBM kernels on a Tesla K40c GPU and a GeForce GTX Titan X (Maxwell GM200) GPU in single and double precision for a grid of size $3 \times 512 \times 512$ lattice nodes. No results for double precision are shown for the Titan X card as this card has only limited hardware support for double precision computations.

References

[1] D. d'Humières, I. Ginzburg, Viscosity independent numerical errors for lattice boltzmann models: From recurrence equations to magic collision numbers, Computers & Mathematics with Applications 58 (5) (2009) 823 – 840, mesoscopic Methods in Engineering and Science. doi:http://dx.doi.org/10.1016/j.camwa.2009.02.008.
URL http://www.sciencedirect.com/science/article/pii/S0898122109000893

[2] D. d'Humières, Generalized lattice boltzmann equations, in: Rarefied Gas Dynamics: Theory and Simulations, Vol. 159 of Progress in Astronautics and Aeronautics, 1992, pp. 450–458.

[3] P. Lallemand, L.-S. Luo, Theory of the lattice Boltzmann method: dispersion, dissipation, isotropy, Galilean invariance, and stability, Physical review. E, Statistical physics, plasmas, fluids, and related interdisciplinary topics 61 (6 Pt A) (2000) 6546–62.

[4] D. d'Humières, I. Ginzburg, M. Krafczyk, P. Lallemand, L.-S. Luo, Multiple-relaxation-time lattice Boltzmann models in three dimensions, Phil. Trans. R. Soc. A 360 (2002) 437–451.

[5] S. Khirevich, I. Ginzburg, U. Tallarek, Coarse-and fine-grid numerical behavior of mrt/trt lattice-boltzmann schemes in regular and random sphere packings, Journal of Computational Physics 281 (2015) 708–742.

[6] I. Ginzbourg, P. M. Adler, Boundary flow condition analysis for the three-dimensional lattice boltzmann model, J. Phys. II France 4 (2) (1994) 191–214. doi:10.1051/jp2:1994123.
URL http://dx.doi.org/10.1051/jp2:1994123

[7] I. Ginzburg, D. dHumières, Multireflection boundary conditions for lattice boltzmann models, Physical Review E 68 (6) (2003) 066614.

[8] I. Ginzburg, F. Verhaeghe, D. d'Humières, Two-relaxation-time lattice boltzmann scheme: About parametrization, velocity, pressure and mixed boundary conditions, Communications in computational physics 3 (2) (2008) 427–478.

[9] I. Ginzburg, D. d'Humières, Multireflection boundary conditions for lattice boltzmann models, Phys. Rev. E 68 (2003) 066614. doi:10.1103/PhysRevE.68.066614.
URL http://link.aps.org/doi/10.1103/PhysRevE.68.066614

[10] F. Dubois, P. Lallemand, M. Tekitek, On a superconvergent lattice boltzmann boundary scheme, Computers & Mathematics with Applications 59 (7) (2010) 2141 – 2149, mesoscopic Methods in Engineering and ScienceInternational Conferences on Mesoscopic Methods in Engineer-

ing and Science. doi:http://dx.doi.org/10.1016/j.camwa.2009.08.055.
URL http://www.sciencedirect.com/science/article/pii/S0898122109006439

[11] F. Dubois, P. Lallemand, Quartic parameters for acoustic applications of lattice boltzmann scheme, Computers & Mathematics with Applications 61 (12) (2011) 3404 – 3416, mesoscopic Methods for Engineering and Science Proceedings of ICMMES-09Mesoscopic Methods for Engineering and Science. doi:http://dx.doi.org/10.1016/j.camwa.2011.01.011.
URL http://www.sciencedirect.com/science/article/pii/S0898122111000162

[12] I. Ginzburg, G. Silva, L. Talon, Analysis and improvement of brinkman lattice boltzmann schemes: Bulk, boundary, interface. similarity and distinctness with finite elements in heterogeneous porous media, Physical Review E 91 (2) (2015) 023307.

[13] I. Ginzburg, Prediction of the moments in advection-diffusion lattice boltzmann method. i. truncation dispersion, skewness, and kurtosis, Phys. Rev. E 95 (2017) 013304. doi:10.1103/PhysRevE.95.013304.
URL http://link.aps.org/doi/10.1103/PhysRevE.95.013304

[14] I. Ginzburg, Prediction of the moments in advection-diffusion lattice boltzmann method. ii. attenuation of the boundary layers via double-Λ bounce-back flux scheme, Phys. Rev. E 95 (2017) 013305. doi:10.1103/PhysRevE.95.013305.
URL http://link.aps.org/doi/10.1103/PhysRevE.95.013305

[15] I. Ginzburg, Equilibrium-type and link-type lattice Boltzmann models for generic advection and anisotropic-dispersion equation, Advances in Water Resources 28 (11) (2005) 1171 – 1195. doi:http://dx.doi.org/10.1016/j.advwatres.2005.03.004.
URL http://www.sciencedirect.com/science/article/pii/S0309170805000874

[16] I. Ginzburg, Truncation errors, exact and heuristic stability analysis of two-relaxation-times lattice boltzmann schemes for anisotropic advection-diffusion equation, Communications in Computational Physics 11 (5) (2012) 14391502. doi:10.4208/cicp.211210.280611a.

[17] I. Ginzburg, Multiple anisotropic collisions for advection–diffusion lattice boltzmann schemes, Advances in Water Resources 51 (2013) 381–404.

[18] M. Geier, M. Schönherr, A. Pasquali, M. Krafczyk, The cumulant lattice boltzmann equation in three dimensions: Theory and validation, Computers & Mathematics with Applications 70 (4) (2015) 507 – 547. doi:http://dx.doi.org/10.1016/j.camwa.2015.05.001.
URL http://www.sciencedirect.com/science/article/pii/S0898122115002126

[19] E. K. Far, M. Geier, K. Kutscher, M. Krafczyk, Distributed cumulant lattice boltzmann simulation of the dispersion process of ceramic agglomerates, J. Comput. Meth. in Science and Engineering 16 (2016) 231–252.

[20] X. Yang, Y. Mehmani, W. A. Perkins, A. Pasquali, M. Schönherr, K. Kim, M. Perego, M. L. Parks, N. Trask, M. T. Balhoff, M. C. Richmond, M. Geier, M. Krafczyk, L.-S. Luo, A. M. Tartakovsky, T. D. Scheibe, Intercomparison of 3d pore-scale flow and solute transport simulation methods, Advances in Water Resources 95 (2016) 176 – 189, pore scale modeling and experiments. doi:http://dx.doi.org/10.1016/j.advwatres.2015.09.015.
URL http://www.sciencedirect.com/science/article/pii/S0309170815002225

[21] E. K. Far, M. Geier, K. Kutscher, M. Krafczyk, Simulation of micro aggregate breakage in turbulent flows by the cumulant lattice boltzmann method, Computers & Fluids 140 (2016) 222 – 231. doi:http://dx.doi.org/10.1016/j.compfluid.2016.10.001.
URL http://www.sciencedirect.com/science/article/pii/S0045793016302936

[22] A. Pasquali, M. Schönherr, M. Geier, M. Krafczyk, Simulation of external aerodynamics of the drivaer model with the lbm on gpgpus, Parallel Computing: On the Road to Exascale (2016) 391–400.

[23] E. Kian Far, M. Geier, K. Kutscher, M. Krafczyk, Implicit large eddy simulation of flow in a micro-orifice with the cumulant lattice boltzmann method, Computation 5 (2) (2017) 23.

[24] M. Geier, A. Pasquali, M. Schönherr, Parametrization of the cumulant lattice boltzmann method for fourth order accurate diffusion part ii: Application to flow around a sphere at drag crisis, Journal of Computational Physics (2017) –doi:https://doi.org/10.1016/j.jcp.2017.07.004.
URL http://www.sciencedirect.com/science/article/pii/S0021999117305065

[25] D. dHumières, M. Bouzidi, P. Lallemand, Thirteen-velocity three-dimensional lattice boltzmann model, Physical Review E 63 (6) (2001) 066702.

[26] J. Tölke, M. Krafczyk, Teraflop computing on a desktop pc with gpus for 3d cfd, International Journal of Computational Fluid Dynamics 22 (7) (2008) 443–456.

[27] A. White, C. Chong, Rotational invariance in the three-dimensional lattice Boltzmann method is dependent on the choice of lattice, Journal of Computational Physics 230 (16) (2011) 6367–6378.

[28] S. K. Kang, Y. A. Hassan, The effect of lattice models within the lattice Boltzmann method in the simulation of wall-bounded turbulent flows, Journal of Computational Physics 232 (1) (2013) 100 – 117. doi:http://dx.doi.org/10.1016/j.jcp.2012.07.023.

[29] S. Geller, S. Uphoff, M. Krafczyk, Turbulent jet computations based on MRT and cascaded lattice Boltzmann models, Computers and Mathematics with Applications 65 (12) (2013) 1956–1966.

[30] M. Geier, A. Greiner, J. G. Korvink, Cascaded digital lattice Boltzmann automata for high reynolds number flow, Phys. Rev. E 73 (2006) 066705. doi:10.1103/PhysRevE.73.066705.

[31] P. Asinari, Generalized local equilibrium in the cascaded lattice Boltzmann method, Phys. Rev. E 78 (2008) 016701. doi:10.1103/PhysRevE.78.016701.
URL http://link.aps.org/doi/10.1103/PhysRevE.78.016701

[32] M. GEIER, A. GREINER, J. G. KORVINK, Properties of the cascaded lattice boltzmann automaton, International Journal of Modern Physics C 18 (04) (2007) 455–462. arXiv:http://www.worldscientific.com/doi/pdf/10.1142/S0129183107010681, doi:10.1142/S0129183107010681.
URL http://www.worldscientific.com/doi/abs/10.1142/S0129183107010681

[33] M. Geier, De-aliasing and stabilization formalism of the cascaded lattice boltzmann automaton for under-resolved high reynolds number flow, INTERNATIONAL JOURNAL FOR NUMERICAL METHODS IN FLUIDS 56 (8) (2007) 1249–1254. doi:10.1002/fld.1634.

[34] A. de Rosis, A central moments-based lattice Boltzmann scheme for shallow water equations, Computer Methods in Applied Mechanics and Engineering 319 (2017) 379–392. doi:10.1016/j.cma.2017.03.001.

[35] F. Dubois, T. Fevrier, B. Graille, On the stability of a relative velocity lattice boltzmann scheme for compressible navier–stokes equations, Comptes Rendus Mécanique 343 (10) (2015) 599–610.
[36] P. L. Bhatnagar, E. P. Gross, M. Krook, A model for collision processes in gases. i. small amplitude processes in charged and neutral one-component systems, Physical review 94 (3) (1954) 511.
[37] A. De Rosis, Non-orthogonal central moments relaxing to a discrete equilibrium: A d2q9 lattice boltzmann model, EPL (Europhysics Letters) 116 (4) (2017) 44003.
[38] A. De Rosis, Nonorthogonal central-moments-based lattice boltzmann scheme in three dimensions, Physical Review E 95 (1) (2017) 013310.
[39] A. De Rosis, Alternative formulation to incorporate forcing terms in a lattice boltzmann scheme with central moments, Physical Review E 95 (2) (2017) 023311.
[40]
[41] W. H. Miller, A treatise on crystallography, For J. & JJ Deighton, 1839.
[42] D. Adams, The Hitchhiker's Guid to the Galaxy, Pan Books, 1979.
[43] P. J. Dellar, Bulk and shear viscosities in lattice boltzmann equations, Phys. Rev. E 64 (2001) 031203. doi:10.1103/PhysRevE.64.031203.
URL http://link.aps.org/doi/10.1103/PhysRevE.64.031203
[44] M. Bouzidi, M. Firdaouss, P. Lallemand, Momentum transfer of a Boltzmann-lattice fluid with boundaries, Physics of Fluids (1994-present) 13 (11) (2001) 3452–3459. doi:http://dx.doi.org/10.1063/1.1399290.
[45] I. Ginzburg, L. Roux, Truncation effect on taylor–aris dispersion in lattice boltzmann schemes: Accuracy towards stability, Journal of Computational Physics 299 (2015) 974–1003.
[46] I. Ginzburg, D. dHumières, A. Kuzmin, Optimal stability of advection-diffusion lattice boltzmann models with two relaxation times for positive/negative equilibrium, Journal of Statistical Physics 139 (6) (2010) 1090–1143.
[47] M. Junk, A. Klar, L.-S. Luo, Asymptotic analysis of the lattice Boltzmann equation, J. Comput. Phys. 210 (2) (2005) 676–704. doi:10.1016/j.jcp.2005.05.003.
[48] F. Dubois, Equivalent partial differential equations of a lattice Boltzmann scheme, Computers & Mathematics with Applications 55 (7) (2008) 1441–1449.
[49] X. He, X. Shan, G. D. Doolen, Discrete boltzmann equation model for nonideal gases, Phys. Rev. E 57 (1998) R13–R16. doi:10.1103/PhysRevE.57.R13.
URL http://link.aps.org/doi/10.1103/PhysRevE.57.R13
[50] P. J. Dellar, An interpretation and derivation of the lattice boltzmann method using strang splitting, Computers & Mathematics with Applications 65 (2) (2013) 129 – 141, special Issue on Mesoscopic Methods in Engineering and Science (ICMMES-2010, Edmonton, Canada). doi:http://dx.doi.org/10.1016/j.camwa.2011.08.047.
URL http://www.sciencedirect.com/science/article/pii/S0898122111007206
[51] D. J. Holdych, D. R. Noble, J. G. Georgiadis, R. O. Buckius, Truncation error analysis of lattice boltzmann methods, Journal of Computational Physics 193 (2) (2004) 595–619.
[52] M. Hénon, Viscosity of a lattice gas, Complex systems 1 (4) (1987) 762–790.
[53] M. Geier, A. Pasquali, Fourth order galilean invariance for the lattice boltzmann method, submitted to Computers and Fluids (2017).
[54] Y. H. Qian, D. d'Humières, P. Lallemand, Lattice BGK Models for Navier-Stokes Equation, Europhysics Letters 17 (6) (1992) 479–484.
[55] P. J. Dellar, Incompressible limits of lattice Boltzmann equations using multiple relaxation times, Journal of Computational Physics 190 (2) (2003) 351 – 370. doi:http://dx.doi.org/10.1016/S0021-9991(03)00279-1.
[56] T. Zeiser, G. Wellein, G. Hager, S. Donath, F. Deserno, P. Lammers, M. Wierse, Optimized lattice boltzmann kernels as testbeds for processor performance, Regional Computing Center of Erlangen (RRZE), Martensstraße 1.
[57] G. Welleina, P. Lammersb, G. Hagera, S. Donatha, T. Zeisera, Towards optimal performance for lattice boltzmann applications on terascale computers, in: Proc. Parallel CFD Conference. Amsterdam: Elsevier, 2006, pp. 31–40.
[58] S. Williams, L. Oliker, J. Carter, J. Shalf, Extracting ultra-scale lattice boltzmann performance via hierarchical and distributed auto-tuning, in: 2011 International Conference for High Performance Computing, Networking, Storage and Analysis (SC), IEEE, 2011, pp. 1–12.
[59] M. Wittmann, T. Zeiser, G. Hager, G. Wellein, Modeling and analyzing performance for highly optimized propagation steps of the lattice boltzmann method on sparse lattices, arXiv preprint arXiv:1410.0412.
[60] C. Feichtinger, J. Habich, H. Köstler, U. Rüde, T. Aoki, Performance modeling and analysis of heterogeneous lattice boltzmann simulations on cpu–gpu clusters, Parallel Computing 46 (2015) 1–13.
[61] T. Ohwada, P. Asinari, D. Yabusaki, Artificial compressibility method and lattice boltzmann method: Similarities and differences, Computers & Mathematics with Applications 61 (12) (2011) 3461 – 3474, mesoscopic Methods for Engineering and Science Proceedings of ICMMES-09Mesoscopic Methods for Engineering and Science. doi:http://dx.doi.org/10.1016/j.camwa.2010.08.032.
URL http://www.sciencedirect.com/science/article/pii/S0898122110005961
[62] P. Asinari, T. Ohwada, E. Chiavazzo, A. F. D. Rienzo, Link-wise artificial compressibility method, Journal of Computational Physics 231 (15) (2012) 5109 – 5143. doi:http://dx.doi.org/10.1016/j.jcp.2012.04.027.
URL http://www.sciencedirect.com/science/article/pii/S0021999112002082
[63] F. Dubois, P. Lallemand, C. Obrecht, M. M. Tekitek, Lattice boltzmann model approximated with finite difference expressions, Computers & Fluids (2016) –doi:http://dx.doi.org/10.1016/j.compfluid.2016.04.013.
URL http://www.sciencedirect.com/science/article/pii/S0045793016301177
[64] P. J. Dellar, Lattice Boltzmann algorithms without cubic defects in Galilean invariance on standard lattices, Journal of Computational Physics 259 (0) (2014) 270 – 283. doi:http://dx.doi.org/10.1016/j.jcp.2013.11.021.
[65] M. Krafczyk, J. Tölke, L.-S. Luo, Large-eddy simulations with a multiple-relaxation-time lbe model, International Journal of Modern Physics B 17 (01n02) (2003) 33–39.
[66] M. Stiebler, M. Krafczyk, S. Freudiger, M. Geier, Lattice Boltzmann large eddy simulation of subcritical flows around a sphere on non-uniform grids, Computers & Mathematics with Applications 61 (12) (2011) 3475 – 3484. doi:http://dx.doi.org/10.1016/j.camwa.2011.03.063.

[67] G. Eitel-Amor, M. Meinke, W. Schröder, A lattice-boltzmann method with hierarchically refined meshes, Computers & Fluids 75 (2013) 127–139.
[68] M. Geier, A. Fakhari, T. Lee, Conservative phase-field lattice boltzmann model for interface tracking equation, Physical Review E 91 (6) (2015) 063309.
[69] A. Fakhari, M. Geier, D. Bolster, A simple phase-field model for interface tracking in three dimensions, Computers & Mathematics with Applications.
[70] A. Fakhari, M. Geier, T. Lee, A mass-conserving lattice boltzmann method with dynamic grid refinement for immiscible two-phase flows, Journal of Computational Physics 315 (2016) 434–457.
[71] F. Dubois, P. Lallemand, Towards higher order lattice boltzmann schemes, Journal of Statistical mechanics: theory and experiment 2009 (06) (2009) P06006.
[72] M. Geier, M. Schönherr, Esoteric twist: An efficient in-place streaming algorithmus for the lattice boltzmann method on massively parallel hardware, Computation 5 (2). doi:10.3390/computation5020019.
URL http://www.mdpi.com/2079-3197/5/2/19
[73] M. Schönherr, Towards reliable les-cfd computations based on advanced lbm models utilizing (multi-) gpgpu hardware, Ph.d. thesis, Technische Universität Braunschweig (2015).